https://doi.org/10.5194/egusphere-2026-3508
Preprint. Discussion started: 31 July 2026

Compound intense warming and precipitation events in the Patagonian Icefields and the Antarctic Peninsula Ice Sheet – Part 1: Event frequency, atmospheric circulation and impacts on glacier surface

Christian Torres[1], Deniz Bozkurt[2,3,4], Vincent Favier[5], Victoire Buffet[5,11], Claudio Bravo[6], Xavier Fettweis[7], Thomas Dethinne[7], Antoine Rabatel[5], Maximiliano Viale[8], Sang-Jong Park[9], Jorge Arigony-Neto[10]

[1]Laboratory of Ocean and Atmosphere Studies (LOA), Earth Observation and Geoinformatics Division (DIOTG), National Institute for Space Research (INPE), São José dos Campos, Brazil
[2]Department of Meteorology, University of Valparaíso, Valparaíso Chile
[3]Center for Climate and Resilience Research, Santiago, Chile
[4]Center for Oceanographic Research COPAS COASTAL, University of Concepción, Concepción, Chile
[5]Univ. Grenoble Alpes, CNRS, IRD, INRAE, Grenoble-INP, Institut des Géosciences de l'Environnement (IGE, UMR 5001), Grenoble, 38000, France
[6]Centro de Estudios Científicos (CECs), Valdivia, Chile
[7]Laboratory of Climatology, Department of Geography, SPHERES research unit, University of Liège, Liège, Belgium
[8]Instituto Argentino de Nivología, Glaciología y Ciencias Ambientales CCT-CONICET, Mendoza, Argentina
[9]Division of Ocean and Atmosphere Sciences, Korea Polar Research Institute, Incheon, South Korea
[10]Institute of Oceanography, Universidade Federal do Rio Grande, Brazil
[11]Biogéosciences, UMR6282 CNRS / Université Bourgogne Europe, Dijon, France

Correspondence to: Christian Torres (christian.ramos@inpe.br)

Abstract. Intense warming events (IWE) and intense precipitation events (IPE) and their impacts on ice bodies remain overlooked. Using in situ observations, a high-resolution regional circulation model and catalogue of atmospheric river (AR) occurrences, we investigate concurrent IWE over the Patagonian Icefields and IPE over the Antarctic Peninsula Ice Sheet associated with landfalling ARs. Our study focuses on summers (November–March) from 1980 to 2022. We identified 127 compound events linked to a dipole circulation pattern characterized by a ridge over southern South America and a low-pressure system over the Bellingshausen Sea. Both regions experience pronounced surface warming and enhanced melt leading to a negative Surface Mass Balance over the Patagonian Icefields, while positive anomalies still prevailed over the Antarctic Peninsula Ice Sheet were related with increased snowfall associated with AR activity. Surface Energy Balance anomalies were mainly driven by enhanced incoming shortwave radiation over Patagonia but increased longwave radiation over the Antarctic Peninsula, whereas sensible heat flux positively contributed in both regions. These findings highlight the interconnected influence of intense events and AR-driven dipole circulation patterns on the Southern Hemisphere cryosphere, even though individual events exhibit substantial thermodynamic variability and distinct life-cycle characteristics.

https://doi.org/10.5194/egusphere-2026-3508
Preprint. Discussion started: 31 July 2026

1 Introduction

The melting of glaciers, icefields, and ice sheets is currently one of the major contributors to global mean sea-level rise. The Patagonian Icefields have the potential to contribute approximately 15 mm to global mean sea level (Fürst et al., 2024), while the Antarctic Peninsula Ice Sheet could contribute around 69 mm (Huss and Farinotti, 2014). Both regions have experienced significant changes in temperature and precipitation patterns in recent decades. In the Patagonian Icefields, observations at Perito Moreno Glacier indicate a warming trend of 0.2 ± 0.1 °C per decade from the mid-1990s to 2020 (Minowa et al., 2023), together with spatially heterogeneous precipitation trends (Garreaud et al., 2013). In the Antarctic Peninsula Ice Sheet, warming has been among the strongest in the Southern Hemisphere reaching 0.44 ± 0.33 °C per decade over 1977–2018 at Rothera station (67.5°S; Turner et al., 2020), although this trend was interrupted by regional cooling between 1999 and 2014 (Turner et al., 2016; Carrasco et al., 2021). Precipitation has also increased across parts of the Antarctic Peninsula, particularly in its northern sector (Carrasco and Cordero, 2020), and combined with regional warming, these changes may shift precipitation from snow to rain and enhance surface melt.

During the same period, glacier mass loss has intensified in both regions. In the Patagonian Icefields, the rate of mass loss increased from 15.1 ± 1.1 Gt yr^{-1} in 1968–1999 (Rignot et al., 2003) to 24.1 ± 1.7 Gt yr^{-1} in 2000–2019 (Minowa et al., 2021). Similarly, in the Antarctic Peninsula Ice Sheet, mass loss rose from 6 ± 13 Gt yr^{-1} in 1997–2002 to 33 ± 16 Gt yr^{-1} in 2012–2017 (The IMBIE team, 2018), with a large fraction of this retreat attributed to subsurface ocean warming (e.g., Cook et al., 2016). These atmospheric and glaciological changes are influenced by both large-scale modes of variability and regional circulation anomalies.

Among the dominant modes of climate variability in the Southern Hemisphere, the El Niño–Southern Oscillation (ENSO) and the Southern Annular Mode (SAM) exert contrasting influences on Patagonia and the Antarctic Peninsula. Positive ENSO phases (ENSO+) can trigger cooler conditions over the Antarctic Peninsula (Li et al., 2021; Wang et al., 2025), whereas they can promote warm and dry conditions over Patagonia when they are associated with positive phases of the SAM (SAM+) (e.g., 2016 mega drought on Patagonia; Garreaud et al., 2013; Garreaud, 2018). In contrast, the positive (negative) phase of the SAM deepens (weakens) the Amundsen–Bellingshausen Seas Low, which is generally associated with warmer and wetter (colder and drier) conditions over the Antarctic Peninsula Ice Sheet, while modulating temperature and precipitation patterns over the Patagonian Icefields toward drier (wetter) conditions (Garreaud et al., 2013; Hosking et al., 2013; Fogt and Marshall, 2020; Macha et al., 2025). Superimposed on these modes of variability, persistent large-scale circulation anomalies – including atmospheric blocking and dipole-like pressure configurations – can amplify regional extreme events independently of ENSO and SAM phases by modifying storm tracks and moisture transport. For example, changes in regional circulation have been linked to cooling trends over the Antarctic Peninsula (Turner et al., 2016), while extreme events can also be triggered by convection anomalies in the central tropical Pacific that activate atmospheric teleconnections (Gorodetskaya et al., 2023).

Previous studies have shown that ENSO and SAM explain only a limited fraction of the long-term surface mass balance (SMB) variability over the Patagonian Icefields (Carrasco et al., 2023; Noël et al., 2025; Collao-Barrios et al., 2026) and the Antarctic Peninsula Ice Sheet (Clem et al., 2022; Torres et al., 2024). Instead, SMB variability is more directly linked to regional atmospheric circulation patterns, including poleward shift of subtropical highs driving glacier mass loss over the Patagonian Icefields (Noël et al., 2025), central tropical Pacific convection controlling surface melt over the Antarctic Peninsula Ice Sheet (Clem et al., 2022), and low-pressure systems over the Drake Passage enhancing winter accumulation in both regions (Carrasco et al., 2023; Torres et al., 2024).

Given their geographic proximity, the Patagonian Icefields and the Antarctic Peninsula Ice Sheet can occasionally be affected by the same large-scale atmospheric systems. Under specific synoptic configurations, these systems can simultaneously alter temperature, precipitation, moisture transport and glaciological surface conditions in both regions, potentially leading to concurrent intense events.

In southern South America, heatwaves and intense warming events (IWEs) have been associated with poleward displacements of anticyclonic systems such as the South Pacific Subtropical Anticyclone and transient migratory highs (Jacques-Coper et al., 2021; Demortier et al., 2021; González-Reyes et al., 2023; Collazo et al., 2024). These systems favor clear skies and enhanced surface warming, and have been linked to the expansion of the Hadley cell (Lu et al., 2007). Transient high-pressure systems over southern South America have been connected to regional heatwaves (Collazo et al., 2024). At the same time, when high-pressure systems are paired with low-pressure systems over the Southern Ocean, they enhance the transport of warm and moist air toward the region. In this situation, atmospheric rivers (ARs) can develop and reach the Patagonian Andes (Viale et al., 2018; Garreaud et al., 2024). As a result, the same atmospheric conditions can be associated with both heatwaves and enhanced moisture transport.

Over the Antarctic Peninsula, high-pressure anomalies over the Drake Passage are frequently associated with atmospheric blocking, which can enhance northerly-warm air advection and promote regional warming (Xu et al., 2021; Clem et al., 2022; Bozkurt et al., 2022, González-Herrero et al., 2022; Gorodetskaya et al., 2023, Bozkurt et al., 2024a). These blocking conditions are often accompanied by ARs, which transport warm and moist air toward the Peninsula (Bozkurt et al., 2018). As a result, ARs exert a dual influence on the regional climate: they contribute substantially to precipitation (rainfall and snowfall), supporting surface mass balance (SMB), but can also promote surface melt and ice-shelf weakening when associated with above-freezing air temperatures during austral summer (Wille et al., 2021, 2022; Maclennan et al., 2022; Torres et al., 2024). Furthermore, previous studies indicate that the formation of an atmospheric dipole, characterized by anticyclonic anomalies over the Malvinas/Falkland Islands and cyclonic anomalies over the Amundsen–Bellingshausen seas, favors the occurrence and persistence of summertime rainfall/snowfall over the northern Antarctic Peninsula (Wang et al., 2021; Wang et al., 2022).

Although previous studies have examined heatwaves, IWEs, and intense precipitation events (IPEs) associated with ARs in each region separately (e.g., Viale et al., 2018; Turner et al., 2019; Collazo et al., 2024; González-Herrero et al., 2022; Gorodetskaya et al., 2023), the simultaneous occurrence of events in the Patagonian Icefields and the Antarctic Peninsula Ice

Sheet has been overlooked, despite these events not being rare and potentially having major impacts on the ice bodies of both regions. Understanding common large-scale circulation patterns can simultaneously influence both regions remains an open question. In this context, this study aims to improve the understanding of these processes along a latitudinal gradient by (1) analysing the frequency of the IWEs over the Patagonian Icefields and IPEs and ARs over the Antarctic Peninsula Ice Sheet, (2) analyzing the synoptic patterns and ARs that drive these events, and (3) evaluating their impacts on meteorological and glaciological conditions. To achieve this, we combine latitudinally distributed in situ observations, high-resolution regional climate model simulations, and reanalysis data to capture both local processes and their link to large-scale atmospheric circulation.

2 Data

2.1 In situ observations

We used observational data from five conventional and automatic weather stations distributed latitudinally across both regions (see Fig. 1 for station locations and Table 1 for station details) to support model verification. In Patagonia, daily maximum temperature records from three stations (Coyhaique, Cochrane, and Torres del Paine), covering the period 1980–2020, were obtained from Aguayo et al. (2024). These data were used to evaluate model ability to identify IWE days.
In the Antarctic Peninsula, daily accumulated precipitation data were obtained from King Sejong Station (1996–2020), located in the northern Antarctic Peninsula (Park et al., 2013), and Palmer Station (1990–2019), located on the western Antarctic Peninsula (Groff, 2025; Palmer Station Research Associate, 2023). These datasets were used to assess the ability of the model to identify IPE days.

https://doi.org/10.5194/egusphere-2026-3508
Preprint. Discussion started: 31 July 2026

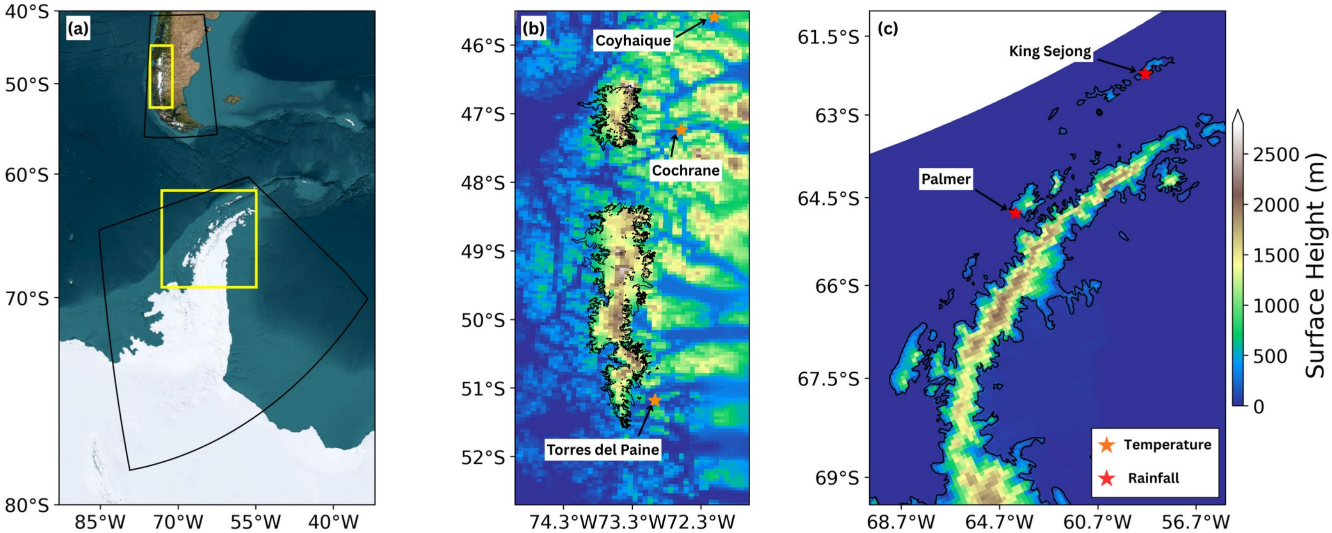

Figure 1: (a) Modèle Atmosphérique Régional (MAR) domains over Patagonia and the Antarctic Peninsula (black polygons). The yellow box indicates the study area encompassing the Patagonian Icefields and the Antarctic Peninsula Ice Sheet. The yellow box over the Antarctic Peninsula highlights the region used to identify atmospheric rivers affecting the area. Panels (b) and (c) show the digital elevation model used in the MAR regional climate simulations. Stars indicate the locations of climatological and automatic meteorological stations.

Table 1. Meteorological stations provide daily maximum temperature and accumulated rainfall data, along with geographic information and periods of record.

Region	**Station**	**Institution**	**Lat. (°); Lon. (°)**	**Ele. (m a.s.l.)**	**Variables measured**	**Period**
Patagonia	Coyhaique	Dirección General de Aguas	45.593°S; 72.108°W	295	Maximum temperature	01/01/1980 – 31/03/2020
	Cochrane	Instituto de Investigaciones Agropecuarias	47.243°S; 72.586°W	201	Maximum temperature	01/01/1980 – 31/03/2020
	Torres Del Paine	Dirección General de Aguas	51.184°S; 72.966°W	241	Maximum temperature	01/01/1980 – 31/03/2020
Antarctic Peninsula	King Sejong	Korea Polar Research Institute	62.230°S; 58.769°W	11	Rainfall	01/01/1996 – 31/12/2020
	Palmer	Antarctic Meteorological Research and Data Center	64.774°S; 64.052°W	10	Rainfall	01/01/1986 – 31/12/2022

2.2 Regional climate model: Modèle Atmosphérique Régional (MAR)

Daily meteorological and glaciological fields at high spatial resolution were obtained from the Modèle Atmosphérique Régional (MAR v3.14 for Patagonia and v3.12 for Antarctic Peninsula), as generated in two previous studies (i.e., Dethinne et al., 2023; Noël et al., 2025). MAR is a regional climate model widely used to investigate the evolution of Greenland and Antarctic ice sheets (Fettweis et al., 2021; Kittel et al., 2022), as well as the Patagonian Icefields (Noël et al., 2025; Collao-Barrios et al., 2026). The model incorporates the Soil Ice Snow Vegetation Atmospheric Transfer (SISVAT, Ridder and Gallée, 1998) surface scheme, which resolves the exchange of energy and mass between the atmosphere and the soil. SISVAT includes a multilayer snow model and a physically based treatment of snow and ice albedo derived from the CROCUS (Brun et al., 1992) snow scheme. The specific calibration and parametrization of the model version used over both areas are also described in Dethinne et al. (2023) and Noël et al. (2025).

The MAR simulations were performed at 5 km spatial resolution over Patagonia and 7.5 km over the Antarctic Peninsula. For both domains, MAR was 6 hourly forced at its lateral and upper (stratosphere) boundary and over the ocean by the ERA5-reanalysis (Herbash et al., 2020). The first few years of simulation are discarded from the result to minimize the impact of the snow model initialisation conditions.

To evaluate meteorological conditions, we used daily air temperature, total precipitation, wind speed, specific humidity and relative humidity. To assess glaciological conditions, we analyzed daily mean of incoming and outgoing shortwave radiation, incoming and outgoing longwave radiation, net radiation, sensible and latent heat fluxes, surface temperature, SMB, surface melt, runoff, and sublimation.

2.3 ERA5 reanalysis

To analyse the dynamical state of the atmosphere during intense events, we used ERA5 reanalysis data (Hersbach et al., 2020). The dynamical analysis was based on mean sea-level pressure (MSLP), 500 hPa geopotential height (Z500), the zonal and meridional wind components at 975 hPa, and the zonal and meridional components of integrated water vapor transport (IVT). The wave flux activity vectors were computed using zonal, meridional and geopotential height at 200 hPa.

3 Methods

3.1 Intense warming and precipitation events detection

We defined a daily IWE when the daily maximum temperature exceeded the 90th percentile of its climatological distribution. Similarly, a daily IPE was identified when total precipitation (rainfall plus snowfall) exceeded the corresponding seasonal 90th percentile (e.g., November–March for the extended summer period).

IWEs and IPEs were identified using MAR outputs only. Following Wang et al. (2022), daily fields of maximum temperature and total precipitation were spatially averaged over all glacierized grid cells within each study region. The

https://doi.org/10.5194/egusphere-2026-3508
Preprint. Discussion started: 31 July 2026

spatial domains corresponded to the Patagonian Icefields and the Antarctic Peninsula Ice Sheet, defined using a binary glacier mask (yellow-bounded areas in Fig. 1), ensuring that only ice-covered grid cells were included in the analysis. The resulting area-averaged time series were used to construct the climatological reference period (1980–2020). For daily maximum temperature, the climatology was derived by applying a harmonic filter to remove the seasonal cycle, followed by a 10-year moving average to account for long-term trends. Seasonal precipitation climatologies were computed over the same period. Events were then identified when the area-averaged daily values exceeded the respective 90th percentile thresholds.

Observations were not used for event identification but exclusively for validation. For this purpose, station measurements of daily maximum temperature and rainfall were compared with MAR values extracted from the nearest grid cell.

For IPE analysis over glacierized regions, total precipitation (rainfall plus snowfall) was considered, whereas only liquid precipitation (rainfall) was used when comparing with in situ observations. This choice was made because precipitation at the observational sites is measured using rain gauges, for which snowfall measurements are associated with substantially uncertainties than rainfall measurements in polar environments, primarily due to wind-induced undercatch and other measurement biases (Souverijns et al., 2017; Seefeldt et al., 2021; Hoover et al., 2021; Dunn et al., 2025).

Percentile-based thresholds have been applied in the region to identify intense events. Previous studies have used thresholds ranging from the 90th to the 99th percentile, including the 90th, 95th, and 99th percentiles (e.g., Turner et al., 2019; Simon et al., 2023; Zhang et al., 2025; Prokhorova et al., 2025). In our study, we used the less restrictive 90th percentile to capture a larger number of events occurring in both regions, but we also tested the more restrictive 95th and 99th percentile to examine its influence on our results.

3.2 Atmospheric River detection over the Antarctic Peninsula

ARs over the Antarctic Peninsula were confirmed using the catalog of Guan and Waliser (2024). The newly refined global AR, named tARgetv4, catalogue described by Guan and Waliser (2024) applies IVT percentile thresholds, using a base threshold above the 85th percentile and a polar-adjusted threshold above the 95th percentile. In addition, it employs geometric IVT criteria (>2,000 km in length and a length-to-width ratio >2) to identify the origin and termination of AR events. tARgetv4 catalogue is based on the ERA5 reanalysis, available from 1940 to 2023 at 6-hourly temporal resolution and 0.25° × 0.25° horizontal resolution.

We adopted the same criterion used by Bozkurt et al. (2024b), in which a given day was classified as an AR day if the AR axis or shape intersected the Peninsula region (73°W–55°W and 61°S–69°S) at least once during the day.

3.3 Atmospheric River detection over the Antarctic Peninsula

Daily anomalies of all atmospheric and glaciological variables from ERA5 or MAR were computed as the difference between the daily value and the climatological mean for the corresponding calendar day, using 1980–2020 as the reference period.

https://doi.org/10.5194/egusphere-2026-3508
Preprint. Discussion started: 31 July 2026

Similar to previous studies (e.g., Welhouse et al., 2016; Garcia-Santos et al., 2025), composite means were calculated for the days classified as IWEs, IPEs, and ARs to quantify the influence of intense events on meteorological and glaciological conditions across the Patagonian Icefields and Antarctic Peninsula Ice Sheet.

3.4 Rossby wave activity

Similar to recent studies (e.g., Liang et al., 2026), we used the Takaya and Nakamura (2001) formulation to examine Rossby wave propagation three days before, during, and after intense compound events, following the equations (1) and (2).

$$W_x = \frac{p\cos(\phi)}{2|U|}\left[\frac{\bar{U}}{a^2\cos^2(\phi)}\left(\left(\frac{\partial\psi}{\partial\lambda}\right)^2 - \psi\frac{\partial^2\psi}{\partial\lambda^2}\right) + \frac{\bar{V}}{a^2\cos(\phi)}\left(\frac{\partial\psi}{\partial\lambda}\frac{\partial\psi}{\partial\phi} - \psi\frac{\partial^2\psi}{\partial\lambda\partial\phi}\right)\right] \quad (1)$$

$$W_y = \frac{p\cos(\phi)}{2|U|}\left[\frac{\bar{U}}{a^2\cos(\phi)}\left(\frac{\partial\psi}{\partial\lambda}\frac{\partial\psi}{\partial\phi} - \psi\frac{\partial^2\psi}{\partial\lambda\partial\phi}\right) + \frac{\bar{V}}{a^2}\left(\left(\frac{\partial\psi}{\partial\phi}\right)^2 - \psi\frac{\partial^2\psi}{\partial\phi^2}\right)\right] \quad (2)$$

Where Wx and Wy represent the zonal and meridional components of the wave activity flux, respectively. The variable ψ corresponds to the geostrophic streamfunction anomaly, while U denotes the horizontal wind magnitude. The terms Ū and V̄ indicate the climatological mean zonal and meridional winds. Latitude and longitude are represented by Φ and λ, respectively, p is the normalized pressure level (pressure divided by 1000 hPa), and a corresponds to the Earth's radius.

4 Results

4.1 MAR data validation

Figure 2 shows the number of IWE and IPE days in each extended summer, based on observations and MAR at five latitudinally distributed stations. High correlations were obtained for IWE (0.59–0.89), indicating good agreement between MAR and observations over Patagonia. For IPE, correlations were moderate (0.45–0.63) over the Antarctic Peninsula. Overall, these results demonstrate that MAR successfully reproduces the intersummer variability of observed intense event frequencies. This skill is further supported at the daily timescale, where high correlations were found between observed and simulated daily maximum temperatures, while moderate correlations were obtained for daily rainfall (Fig. S1).

https://doi.org/10.5194/egusphere-2026-3508
Preprint. Discussion started: 31 July 2026

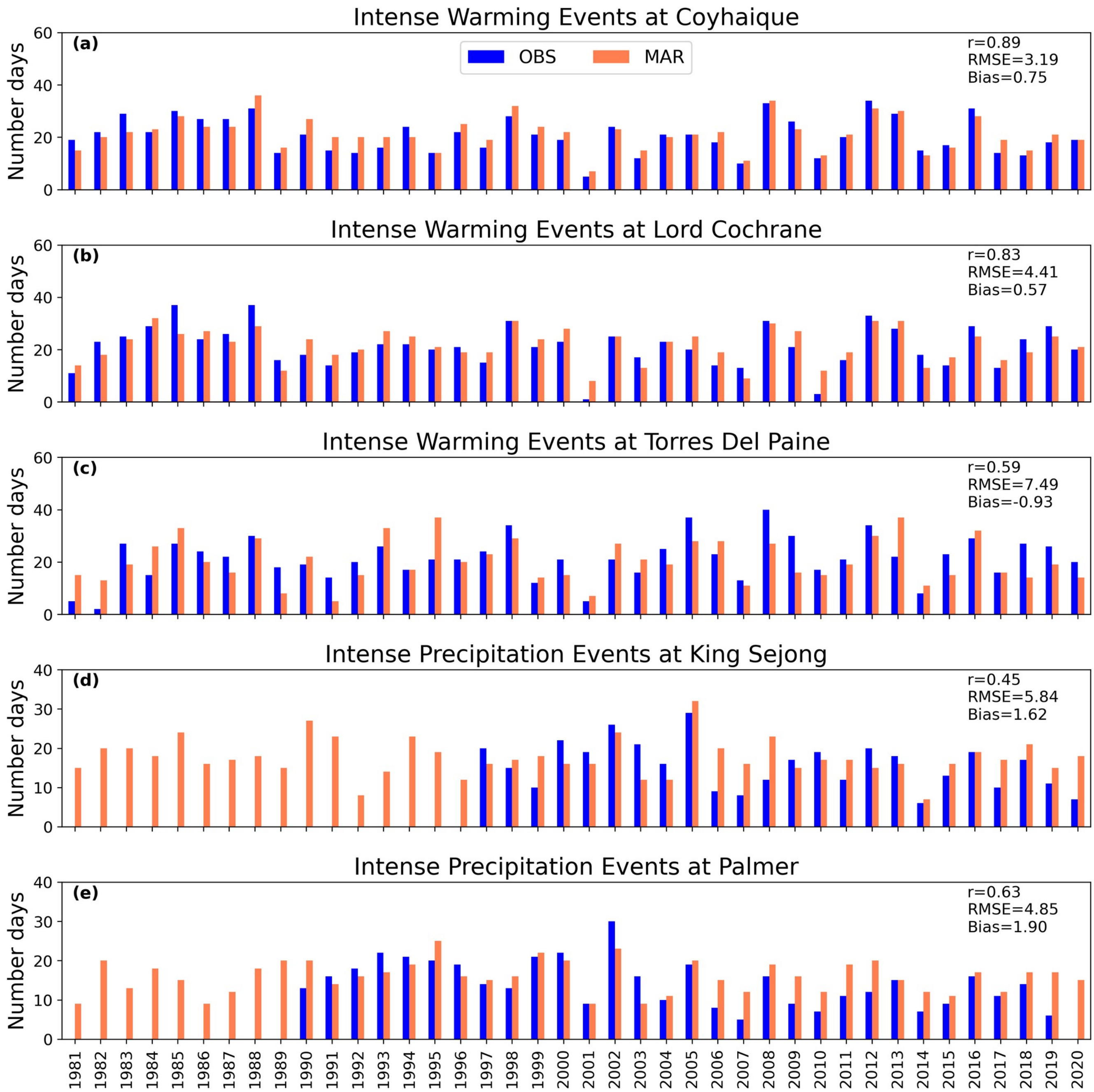

Figure 2: Comparison of the number of IWE and IPE days during extended summer from 1981 to 2020 identified from in situ observations and the nearest MAR grid cell.

https://doi.org/10.5194/egusphere-2026-3508
Preprint. Discussion started: 31 July 2026

4.2 Co-occurrence of intense events and their atmospheric synoptic configuration

Figure 3 shows the number of occurrences of IWE, IPE, and ARs for each extended summer during 1980–2022, identified from spatially averaged daily maximum temperature and total precipitation time series using the criteria described in Sect. 3.1.

IWE occurrence over the Patagonian Icefields exhibits pronounced interannual variability (Fig. 3a), with values ranging from 5 to 40 days per summer. Likewise, the number of IPE days over the Antarctic Peninsula Ice Sheet varies substantially from summer to summer (Fig. 3b), spanning from 10 to 30 days, and is closely associated with the presence of ARs (r=0.74 and p-value<0.01, annual count of IPE and AR days). When considering the simultaneous co-occurrence of IWE, IPE, and ARs over both regions, the number of compound events is limited to at most 10 days per summer (Fig. 3c), indicating that such concurrent events are relatively less common across the study region.

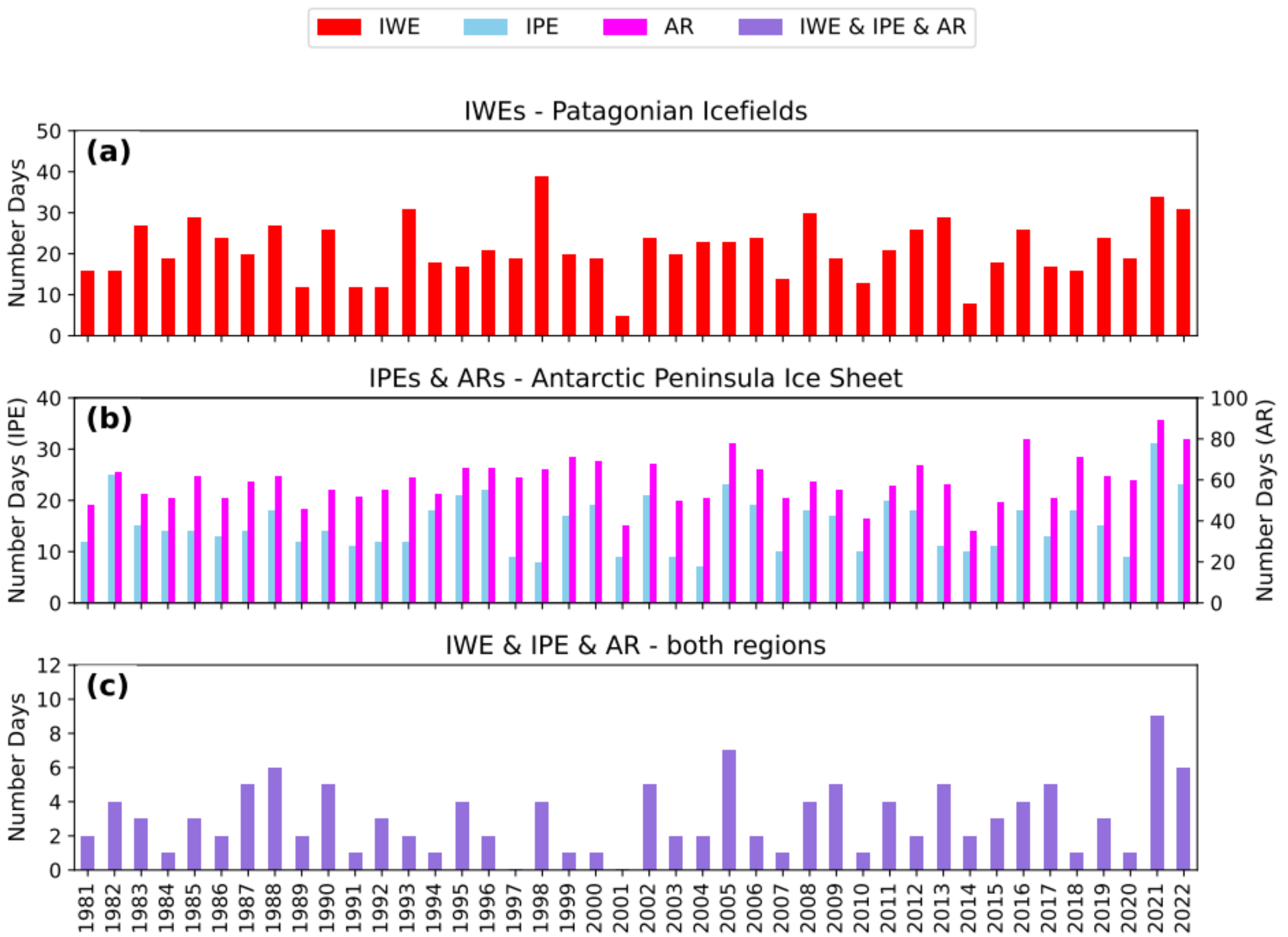

Figure 3: Extended summer occurrence of (a) intense warming event (IWE) over the Patagonian Icefields; (b) intense precipitation event (IPE) and ARs from Guan and Waliser (2024) catalogue affecting the Antarctic Peninsula Ice Sheet; and (c) co-occurring IWE, IPE, and AR across both regions.

https://doi.org/10.5194/egusphere-2026-3508
Preprint. Discussion started: 31 July 2026

Adding all extended-summer over the 1980-2022 period, a total of 910 IWE days were identified over the Patagonian Icefields, associated with the persistent presence of a high-pressure system over the Patagonian region (Fig. 4a). In parallel, 648 days with IPE were detected over the Antarctic Peninsula Ice Sheet, linked to a dipole configuration characterized by a low-pressure system over the Bellingshausen Sea and a high-pressure system over the Falkland Islands (Fig. 4b). The co-occurrence of IWE over the Patagonian Icefields and IPE over the Antarctic Peninsula Ice Sheet was identified on 127 days during the analyzed period. Notably, all of these co-occurring events coincided with the presence of ARs from the tARgetv4 catalogue (Guan and Waliser, 2024), and their simultaneous occurrence was associated with an enhanced IPE dipole pattern (Fig. 4c). Consistent with their association with large-scale atmospheric circulation anomalies, a frequency histogram analysis of compound IWE–IPE events as a function of their spatial extent indicates that these events are not dominated by locally confined anomalies, but rather reflect large-scale atmospheric conditions affecting substantial portions of both regions (Fig. S2).

In terms of duration, 80% of these events last only one day, 16% persist for two days, and the remaining 4% extend to three or more days, indicating that most compound events are short-lived. This prevalence of short-lived events suggests that these episodes are driven by transient synoptic-scale disturbances, likely linked to the rapid passage of Ars.

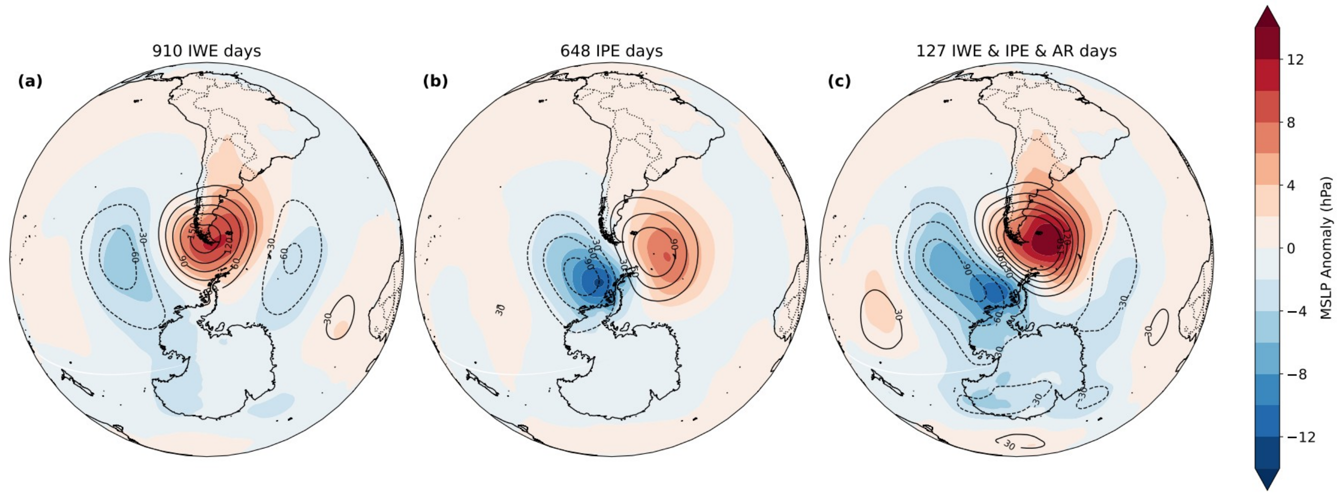

Figure 4: Composite MSLP anomalies (shading) and Z500 anomalies (contours; solid for positive and dashed for negative values, at 25-m intervals) for: (a) IWE days over the Patagonian Icefields (PIs); (b) IPE days affecting the Antarctic Peninsula Ice Sheet (APIS); and (c) days with co-occurring IWEs, IPEs, and ARs across both regions. Anomalies were calculated relative to the 1980–2020 climatological period using ERA5 reanalysis data.

The synoptic evolution from three days before to three days after the compound events indicates that the dipole pattern emerged from a Rossby wave train characterized by alternating high- and low-pressure anomalies over the South Pacific Ocean (Fig. 5). Using the Takaya and Nakamura (2001) formulation (see Sect. 3.4), the associated wave activity flux vectors reveal a clear downstream propagation of wave energy from the South Pacific toward southern South America and the South Atlantic, supporting the interpretation of a propagating Rossby wave train. Prior to the simultaneous IWE and IPE establishment, the high-pressure component of the dipole was located over the eastern Pacific, approximately parallel to the

https://doi.org/10.5194/egusphere-2026-3508
Preprint. Discussion started: 31 July 2026

Patagonian Icefields. During the following two days, the wave train amplified and progressively shifted eastward, while the wave activity flux became increasingly focused over southern South America. The anticyclonic center subsequently intensified and propagated eastward, whereas a cyclonic anomaly deepened over the southern Pacific Ocean and migrated southeastward. Near the mature phase of the events, the dipole structure became strongly amplified and quasi-stationary, suggesting regional accumulation of wave activity and enhanced persistence of the large-scale circulation pattern.

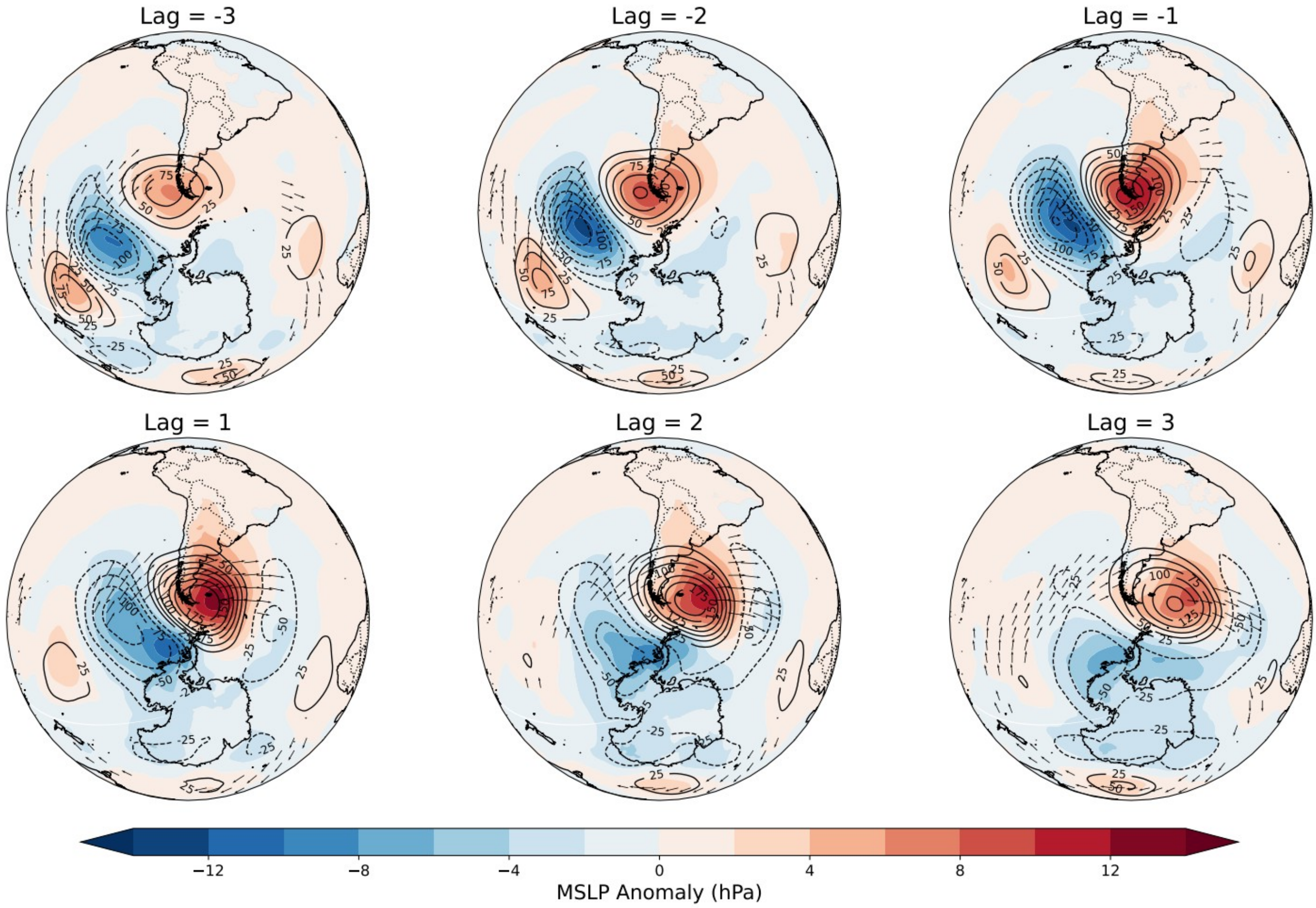

Figure 5: Composite anomalies of MSLP (shading) and Z500 (contours; solid for positive and dashed for negative anomalies, every 25 m) for the 127 identified events, shown from day −3 to day +3 relative to the event onset. Vectors represent wave activity flux anomalies (only present values ≥ 0.1 $m^2 s^{-2}$) at the level of 200 hPa derived from the formulation of Takaya and Nakamura (2001).

4.3 Near-surface atmospheric variables conditions

The spatial distribution of mean daily anomalies in near-surface air temperature, total precipitation, wind speed, specific humidity, and relative humidity was analyzed from MAR outputs to assess the atmospheric conditions during the 127 days with concurrent IWE, IPE and AR during 1980–2022.

https://doi.org/10.5194/egusphere-2026-3508
Preprint. Discussion started: 31 July 2026

For the Patagonian Icefields, the results show positive air temperature anomalies over the entire Patagonian Icefields of up to +8 °C (Fig. 6a), accompanied by generalized negative anomalies in total precipitation reaching −40 mm day⁻¹ (Fig. 6b) and moderate negative anomalies in wind speed of up to −5 m s⁻¹ (Fig. 6c). In contrast, over the entire Antarctic Peninsula Ice Sheet, generalized positive air temperature anomalies reaching +8 °C are observed (Fig. 6d), together with positive anomalies in total precipitation reaching +40 mm day⁻¹ (Fig. 6e) and wind speed anomalies of up to +10 m s⁻¹ (Fig. 6f).

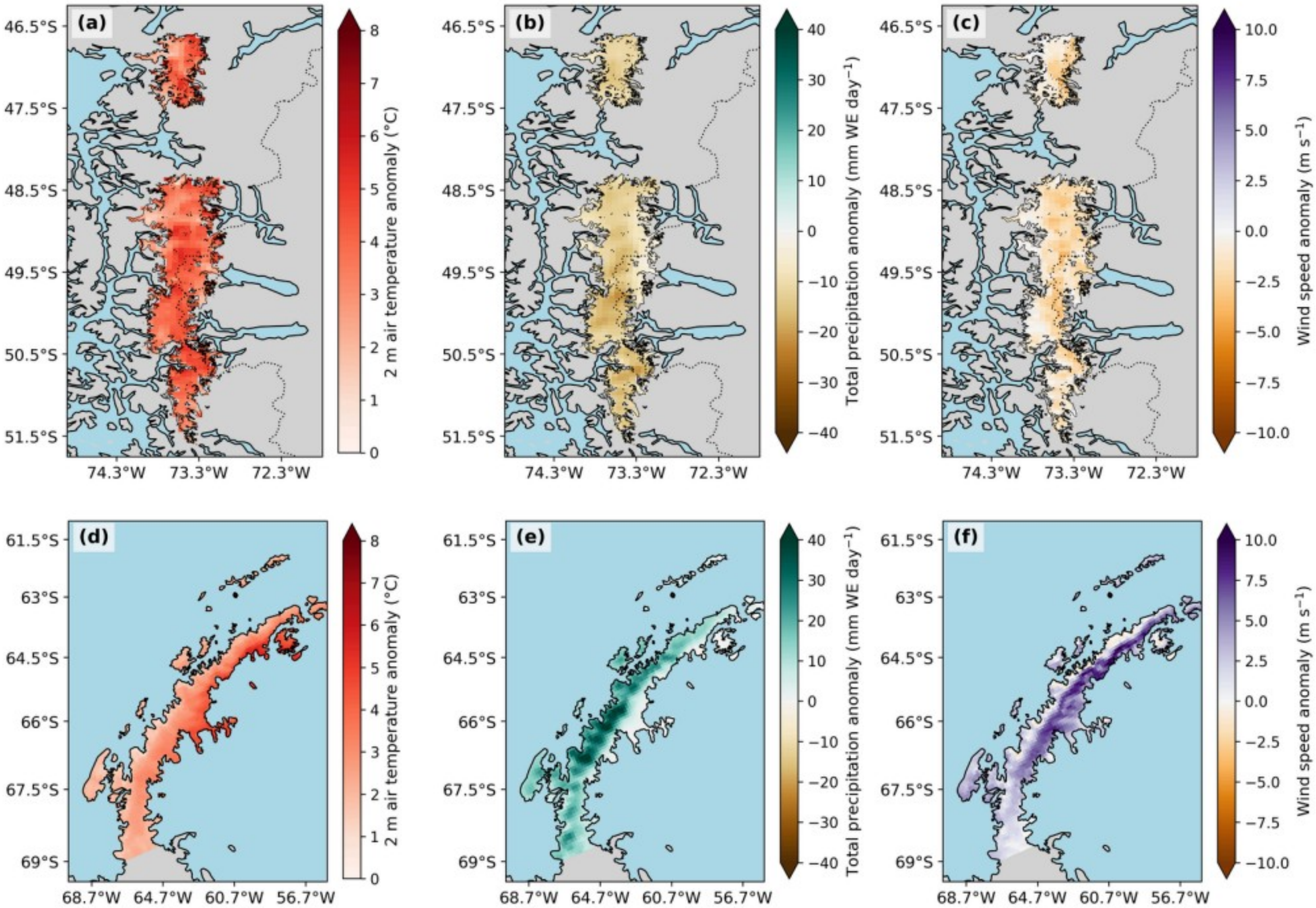

Figure 6: Mean daily anomaly fields of (a, d) 2 m air temperature; (b, e) total precipitation; and (c, f) wind speed for the 127 days identified between November and March over the 1980–2022 period; derived from MAR simulations. Panels (a–c) correspond to the Patagonian Icefields, and panels (d–f) to the Antarctic Peninsula Ice Sheet.

Over the Patagonian Icefields, specific humidity presents a pronounced west–east contrast, characterized by alternating negative and positive anomalies, whereas relative humidity is dominated by negative anomalies (Fig. S3a and b). The negative precipitation anomalies in this region are consistent with the deficit in relative humidity, indicating limited atmospheric moisture availability. In contrast, the alternating negative and positive anomalies in specific humidity are primarily driven by strong temperature anomalies, which modulate the atmospheric moisture-holding capacity. Conversely, over the Antarctic Peninsula Ice Sheet, positive specific humidity anomalies are dominant, and relative humidity exhibits a

https://doi.org/10.5194/egusphere-2026-3508
Preprint. Discussion started: 31 July 2026

clear zonal gradient (Fig. S3d and e). In this region, precipitation variability is also closely linked to relative humidity, with spatial differences in saturation contributing to the observed patterns.

4.4 Glacier surface energy and mass balance conditions

The spatial distribution of mean daily anomalies of net radiation, sensible and latent heat fluxes, SMB, surface melt, sublimation and surface temperature were also analyzed using MAR model outputs to characterize the glaciological conditions during these 127 days.

For the Patagonian Icefields, net radiation exhibits positive anomalies of up to +32 W m⁻² (Fig. 7a), primarily concentrated at lower elevations, whereas high elevations present negative anomalies, indicating a pronounced altitudinal dependence. The SEB is further enhanced by positive anomalies in sensible heat flux reaching up to +142 W m⁻² over large portions of the ice field (Fig. 7b), whereas latent heat flux displays positive anomalies of up to +43 W m⁻² in the eastern sector and negative anomalies of up to −26 W m⁻² in the western sector (Fig. 7c).

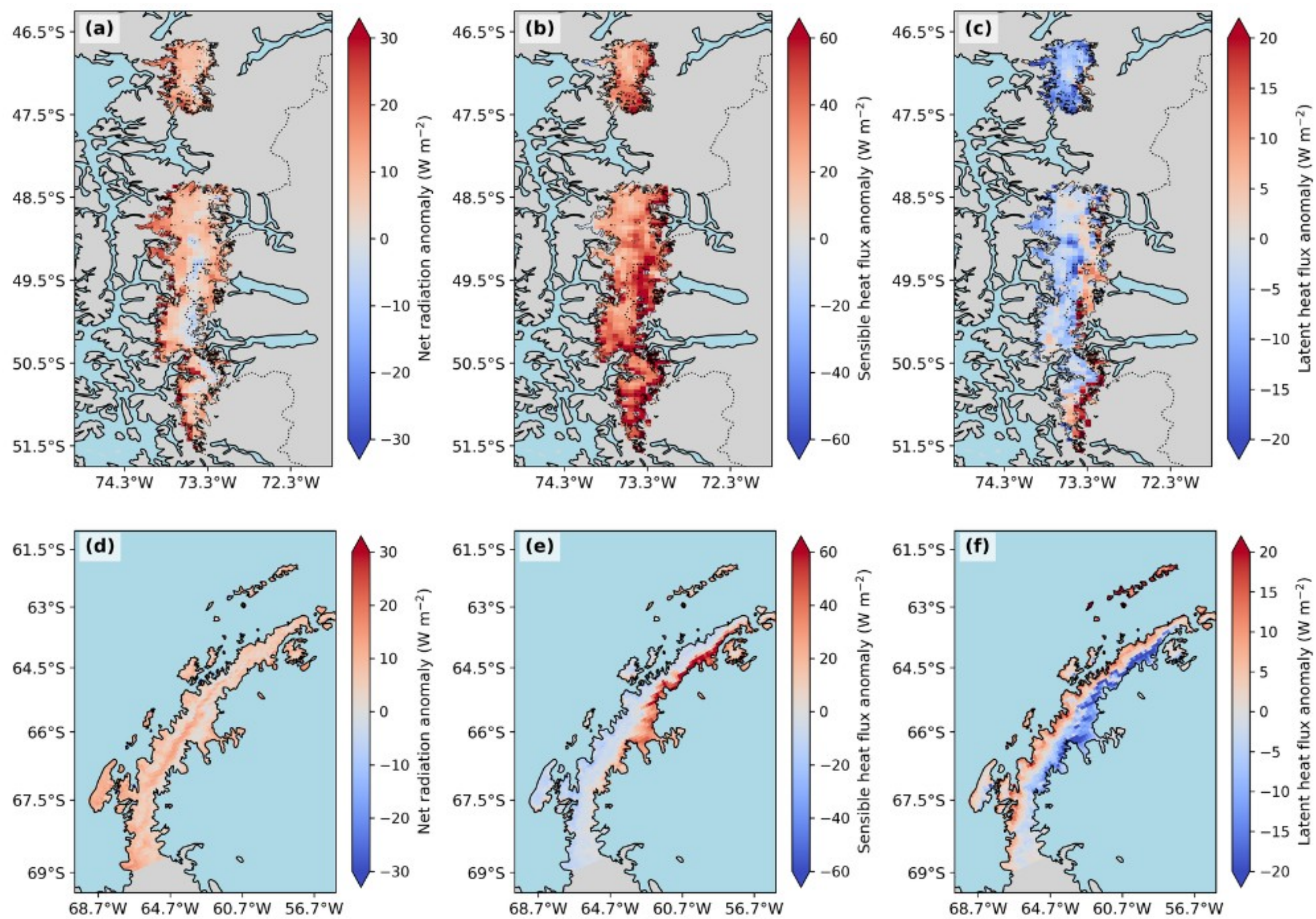

https://doi.org/10.5194/egusphere-2026-3508
Preprint. Discussion started: 31 July 2026

Figure 7: Mean daily anomaly fields of (a, d) net radiation; (b, e) sensible heat flux; and (c, f) latent heat flux for the 127 days identified between November and March over the 1980–2022 period, derived from MAR simulations. Panels (a–c) correspond to the Patagonian Icefields, and panels (d–f) to the Antarctic Peninsula Ice Sheet.

For the Antarctic Peninsula Ice Sheet, net radiation also shows generalized positive anomalies across much of the ice sheet, with values reaching up to +18 W m^{-2} (Fig. 7d). In contrast, sensible heat flux (Fig. 7e) and latent heat flux (Fig. 7f) exhibit a marked west–east spatial variability. Sensible heat flux anomalies of up to +123 W m^{-2} are concentrated in the eastern sector of the Antarctic Peninsula Ice Sheet, reflecting the influence of foehn winds, whereas latent heat flux anomalies of up to +26 W m^{-2} are found in the western sector. Positive surface temperature anomalies are confined to the higher-elevation areas of the Patagonian Icefields (Fig. S3c), while over the Antarctic Peninsula Ice Sheet they are spatially extensive, affecting the entire ice sheet (Fig. S3f).

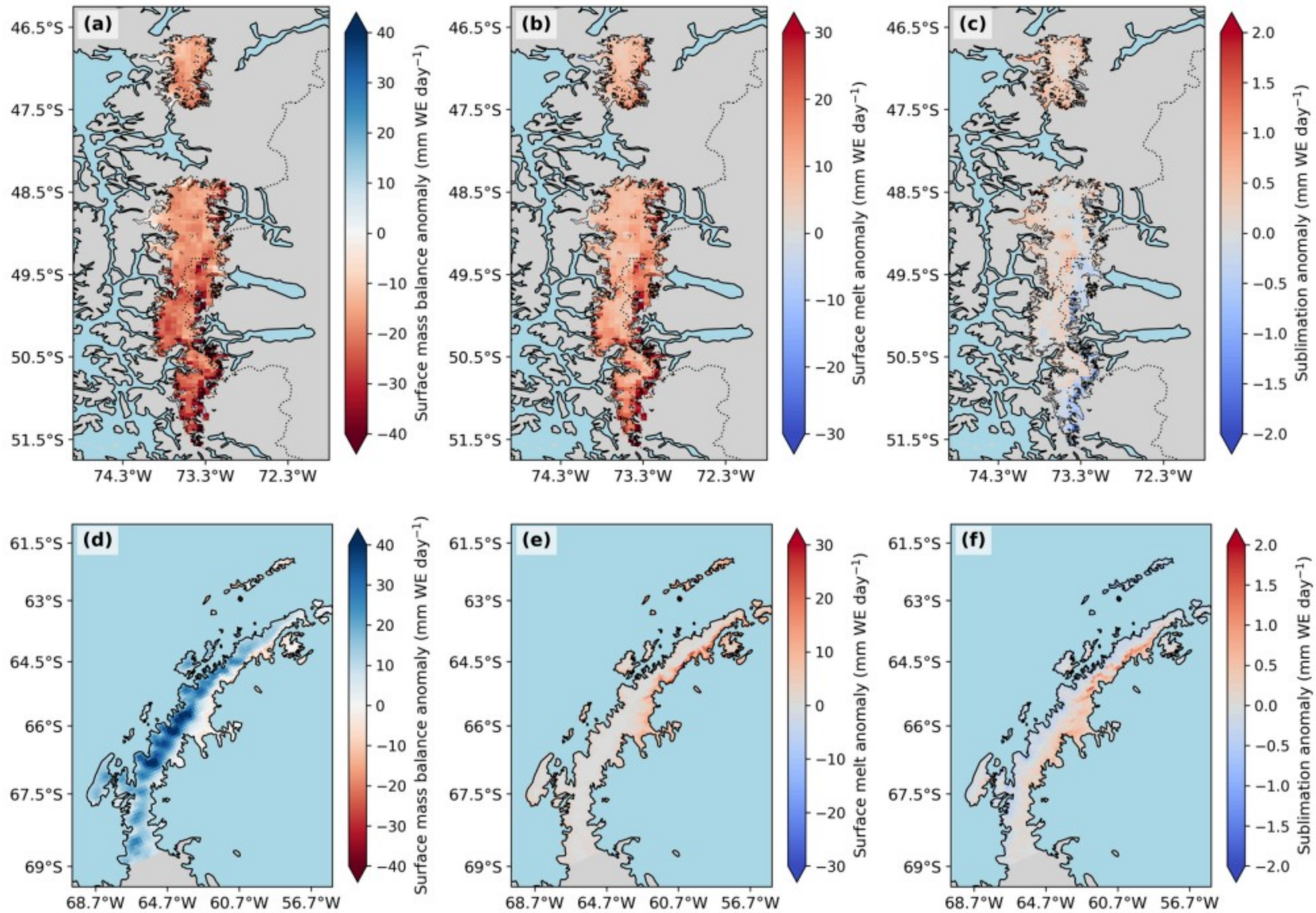

Figure 8: Mean daily anomaly fields of (a, d) SMB; (b, e) surface melt; and (c, f) sublimation for the 127 days identified between November and March over the 1980–2022 period, derived from MAR simulations. Panels (a–c) correspond to the Patagonian Icefields, and panels (d–f) to the Antarctic Peninsula Ice Sheet.

Regarding SMB, the Patagonian Icefields exhibit negative anomalies across the entire ice field (Fig. 8a), whereas the Antarctic Peninsula Ice Sheet shows positive anomalies over the western sector, but slightly negative anomalies over the low-elevation eastern sector and the South Shetland Islands (Fig. 8d). In the whole Patagonian Icefields and eastern Antarctic Peninsula Ice Sheet sector, positive anomalies in surface melt were observed, reaching values of up to ~30 mm w.e. day^{-1} (Fig. 8b, e). In contrast, sublimation displays pronounced spatial variability, with negative anomalies over the eastern sector of the Patagonian Icefields and the western sector of the Antarctic Peninsula Ice Sheet—indicative of deposition—and positive anomalies over the western sector of the Patagonian Icefields and the eastern sector of the Antarctic Peninsula Ice Sheet (Fig. 8c, f).

Table 2 summarizes the atmospheric and glaciological conditions associated with the 127 identified compound-event days. During these events, air temperature increases on average by +3.97 °C over the Patagonian Icefields and by +2.76 °C over the Antarctic Peninsula Ice Sheet. In contrast, total precipitation decreases by up to −12.50 mm day^{-1} over the Patagonian Icefields, while increasing by up to +13.92 mm day^{-1} over the Antarctic Peninsula Ice Sheet. Consistent with these precipitation anomalies, wind speed and relative humidity decrease over the Patagonian Icefields, reflecting drier atmospheric conditions, whereas both variables increase over the Antarctic Peninsula Ice Sheet, indicating enhanced moisture transport associated with atmospheric river activity.

These contrasting atmospheric conditions are reflected in the SEB. Over the Patagonian Icefields, enhanced incoming shortwave radiation (+45.51 W m^{-2}) and sensible heat flux (+39.74 W m^{-2}) provide the main positive energy contributions, consistent with reduced cloud cover and warmer near-surface conditions. In contrast, over the Antarctic Peninsula Ice Sheet, the dominant positive contributions arise from increased incoming longwave radiation (+31.55 W m^{-2}) and sensible heat flux (+6.76 W m^{-2}), reflecting the presence of warm, moist air masses and enhanced cloudiness.

The resulting SMB response differs markedly between the two regions. Over the Patagonian Icefields, the combination of reduced precipitation and enhanced melt leads to a negative SMB anomaly of −18.68 mm w.e. day^{-1}. In contrast, the Antarctic Peninsula Ice Sheet exhibits a positive SMB anomaly of +10.98 mm w.e. day^{-1}, indicating that increased snowfall more than compensates for melt losses at the regional scale. Nevertheless, surface melt increases in both regions (+12.66 mm w.e. day^{-1} over the Patagonian Icefields and +3.56 mm w.e. day^{-1} over the Antarctic Peninsula Ice Sheet), accompanied by enhanced runoff (+7.01 and +2.06 mm w.e. day^{-1}, respectively). This response varies with elevation: over the Antarctic Peninsula Ice Sheet, low-elevation areas exhibit a negative SMB anomaly (−1.44 mm w.e. day^{-1}), indicating net mass loss during these events despite the positive SMB observed at the ablation zone.

https://doi.org/10.5194/egusphere-2026-3508
Preprint. Discussion started: 31 July 2026

Table 2. Daily anomalies of atmospheric and glaciological variables derived from MAR, spatially averaged over the Patagonian Icefields (PIs) and Antarctic Peninsula Ice Sheet (APIS) for the 127 analyzed days. Anomalies are computed relative to the 1981–2020 daily climatology. Whole refers to the entire glacierized area, Low denotes the lower-elevation regions based on the equilibrium-line altitude, and West and East indicate the western and eastern sectors of each region, respectively. For each region, we determined the equilibrium line altitude based on the annual SMB climatology using MAR data.

		Whole		**Low**		**West**		**East**	
	Units	**PIs**	**APIS**	**PIs**	**APIS**	**PIs**	**APIS**	**PIs**	**APIS**
Air temperature	°C	3.71	2.75	3.21	2.88	3.51	2.08	3.88	3.56
Total precipitation	mm w.e.	-11.57	13.04	-9.84	4.87	-12.31	16.22	-11.06	9.17
Wind speed	m s^{-1}	-1.45	3.27	-0.85	2.62	-1.03	2.30	-1.83	4.45
Relative humidity	%	-17.21	3.08	-16.38	-0.21	-18.09	6.70	-16.48	-1.34
Incoming shortwave radiation	W m^{-2}	45.51	-62.85	50.85	-56.67	63.90	-83.61	30.05	-37.54
Outgoing shortwave radiation	W m^{-2}	-21.51	51.10	-21.81	44.77	-34.45	66.49	-10.73	32.32
Incoming longwave radiation	W m^{-2}	-9.59	31.55	-9.90	30.66	-12.79	35.85	-7.02	26.30
Outgoing longwave radiation	W m^{-2}	-4.39	-12.68	-2.60	-10.68	-3.10	-11.52	-5.52	-14.09
Net radiation	W m^{-2}	10.01	7.11	16.54	8.08	13.56	7.20	6.78	6.99
Sensible heat flux	W m^{-2}	38.74	6.76	37.51	19.81	30.63	-3.40	45.50	19.16
Latent heat flux	W m^{-2}	-2.94	0.21	-1.74	6.92	-5.77	6.34	-0.67	-7.27
Surface mass balance	mm w.e.	-18.68	10.98	-18.29	-1.44	-16.93	14.42	-20.08	6.77
Surface melt	mm w.e.	12.66	3.56	14.29	8.47	10.49	2.46	14.32	4.90
Sublimation	mm w.e.	0.11	-0.01	0.10	-0.22	0.20	-0.20	0.03	0.22
Runoff	mm w.e.	7.01	2.06	8.40	6.50	4.43	1.98	8.99	2.16

In terms of impact, simultaneous events contribute up to ~10 % of total ablation over the Patagonian Icefields, while their contribution to accumulation remains negligible (Fig. 9a), indicating that their impact in Patagonia is primarily through enhanced ablation. In contrast, over the Antarctic Peninsula Ice Sheet, these events account for up to ~20 % of total

https://doi.org/10.5194/egusphere-2026-3508
Preprint. Discussion started: 31 July 2026

accumulation and less than 15 % of ablation (Fig. 9b), highlighting a comparative influence on both accumulation and ablation across the peninsula.

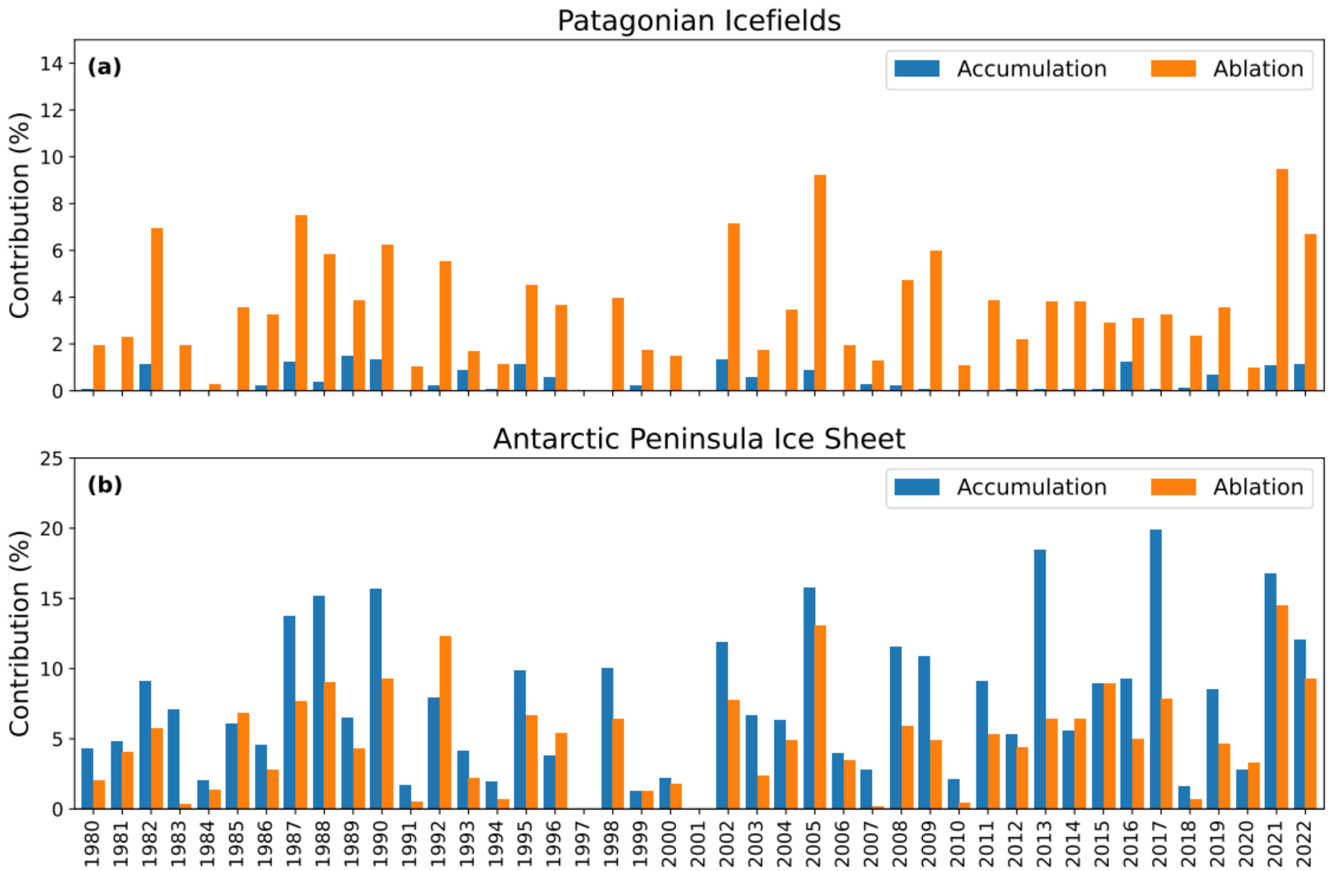

Figure 9: Percentage contribution to total accumulation and ablation for (a) the Patagonian Icefields and (b) the Antarctic Peninsula Ice Sheet during the 127 identified day events.

4.5 Atmospheric river impacts on the conditions at the glaciers' surface

We analyzed the impact of ARs on surface conditions over the Antarctic Peninsula Ice Sheet during 577 IPE–AR events and 127 compound IWE–IPE–AR events. Events were classified according to the 75th percentile of IVT, separating them into low-IVT and high-IVT categories. This threshold was selected to isolate the most intense IVT AR conditions while maintaining sufficiently large sample sizes for statistical comparisons. Differences between the two subgroups were evaluated using the Mann–Whitney U test, and effect sizes were quantified using Cliff's delta.

Of the 577 IPE–AR events identified over the Antarctic Peninsula Ice Sheet, 426 were classified as low-IVT and 151 as high-IVT events. Composite analyses reveal statistically significant differences in near-surface air temperature, incoming longwave radiation, outgoing longwave radiation, and surface melt between the two IVT categories (Table 3). High-IVT events are associated with lower air temperatures, lower incoming longwave radiation, higher outgoing longwave radiation,

https://doi.org/10.5194/egusphere-2026-3508
Preprint. Discussion started: 31 July 2026

and reduced surface melt. However, effect-size estimates indicate that these differences are generally small (|Cliff's delta| ≈ 0.17–0.22). Most atmospheric, radiative, and surface mass balance variables do not exhibit statistically significant differences between low- and high-IVT events. In particular, precipitation anomalies do not differ significantly between the two groups, suggesting that precipitation magnitude during IPE–AR events is not controlled solely by IVT intensity and may also depend on AR geometry, orientation, and the associated synoptic-scale circulation.

The 127 compound IWE–IPE–AR events were divided into 95 low-IVT and 32 high-IVT cases. Significant differences were detected in near-surface air temperature, wind speed, relative humidity, sensible heat flux, and surface melt. Compared to low-IVT events, high-IVT compound events are characterized by lower air temperatures, weaker winds, higher relative humidity, lower sensible heat flux, and reduced surface melt. Cliff's delta values indicate small effect sizes for all significant variables (|Cliff's delta| ≈ 0.23–0.32). In contrast, precipitation anomalies, radiative fluxes, net radiation, and surface mass balance components do not exhibit statistically significant differences between the two IVT categories. These findings suggest that the atmospheric and glaciological response during compound IWE–IPE–AR events is governed primarily by the large-scale dipole circulation pattern associated with these events, while IVT intensity plays a secondary role.

Overall, the results indicate that increasing IVT intensity within already selected precipitation-enhanced AR events produces only modest changes in surface meteorological and glaciological conditions. Although various variables exhibit statistically significant differences, the associated effect sizes remain small, indicating that IVT intensity explains only a limited fraction of the variability in Antarctic Peninsula Ice Sheet surface conditions once the occurrence of IPE–AR or IWE–IPE–AR events has been established. These results suggest that the occurrence and large-scale dipole circulation of the events are more important than IVT magnitude alone in shaping atmospheric, energy-balance, and surface mass-balance anomalies over the Antarctic Peninsula Ice Sheet.

*Table 3. Impact of ARs intense on surface conditions over the Antarctic Peninsula Ice Sheet during IPE–AR days and compound days (IWE+IPE+AR) events, classified into low-IVT and high-IVT categories. Significance is indicated by number asterisk, where * ($p < 0.05$).*

		IPE+AR			IWE+IPE+AR		
	Units	Low-IVT	High-IVT	Cliff's delta	Low-IVT	High-IVT	Cliff's delta
Air temperature	°C	2.02	1.29*	small	2.98	2.06*	small
Total precipitation	mm w.e.	11.15	11.48	negligible	13.09	12.91	negligible
Wind speed	m s^{-1}	2.76	2.48	negligible	3.51	2.54*	small
Relative humidity	%	3.71	3.79	negligible	2.69	4.22*	small
Incoming shortwave radiation	W m^{-2}	-58.38	-54.56	negligible	-65.70	-54.40	small
Outgoing shortwave radiation	W m^{-2}	47.36	43.46	negligible	53.67	43.46	small

https://doi.org/10.5194/egusphere-2026-3508
Preprint. Discussion started: 31 July 2026

Incoming longwave radiation	W m⁻²	30.14	27.16*	small	32.31	29.28	negligible
Outgoing longwave radiation	W m⁻²	-10.59	-8.06*	small	-13.23	-11.05	small
Net radiation	W m⁻²	8.53	8.01	negligible	7.05	7.29	negligible
Sensible heat flux	W m⁻²	2.18	0.68	negligible	8.06	2.92*	small
Latent heat flux	W m⁻²	-1.44	-1.62	negligible	0.08	0.60	negligible
Surface mass balance	mm w.e.	9.53	9.97	negligible	11.03	10.83	negligible
Surface melt	mm w.e.	2.28	1.62*	small	3.84	2.74*	small
Sublimation	mm w.e.	0.04	0.05	negligible	-0.01	-0.02	negligible
Runoff	mm w.e.	1.56	1.45	negligible	2.04	2.10	negligible

5 Discussion

5.1 MAR and method validation

We compared several MAR variables with outputs from physically based glaciological models previously reported for both regions (Bravo et al., 2022; Torres et al., 2024, 2025). A key advantage of these studies is the use of in situ meteorological observations to force the models, as well as their higher spatial resolution (e.g., ~200 m over the southern Patagonian Icefields). Despite these methodological differences, MAR reproduces the main meteorological variables and SEB components consistently with previous studies (Figs. S4–7). The discrepancies observed in sensible and latent heat fluxes likely reflect differences in parameterization schemes rather than direct effects of spatial resolution. Overall, these results support the use of MAR outputs to robustly identify and characterize intense warming and precipitation events.

The identification of IWEs and IPEs was primarily based on outputs from MAR. To evaluate the reliability of the detected events, we compared the number of IWEs and IPEs with available observations of daily maximum temperature from three stations in Patagonia and daily accumulated rainfall in the Antarctic Peninsula, using values extracted from the nearest MAR grid cell to each station. Intersummer correlations between IWE days identified by the model and the observations range from moderate to high, with significantly higher values at lower latitudes. These results indicate that MAR robustly captures the intersummer variability of IWE episodes in the region, consistent with previous studies showing that regional models and reanalysis products can skillfully represent intense warming events (e.g., Demortier et al., 2021).

For IPEs, correlations are moderate at the two stations (i.e., King Sejong and Palmer) on the Antarctic Peninsula. Precipitation at these stations is measured using rain gauges, which are known to have substantial uncertainties when measuring snowfall. Therefore, only liquid precipitation (rain) from MAR is used in the comparison. The comparison is performed for all available observation days and is not restricted to days when MAR simulates rainfall. This moderate agreement likely reflects well-known limitations associated with precipitation measurements in polar environments (Souverijns et al., 2017; Seefeldt et al., 2021; Hoover et al., 2021; Dunn et al., 2025). Thus, precipitation measurements in polar regions should generally be interpreted with caution. In particular, gauge measurements are subject to undercatchment under strong wind conditions, as turbulence can prevent hydrometeors from entering the gauge, an effect that is especially pronounced for snowfall (Hoover et al., 2021). Previous studies have shown that even advanced gauges may fail to capture snowfall when wind speeds exceed ~5 m s^{-1}, particularly at low temperatures (Dunn et al., 2025). In addition, strong winds —frequent over the Antarctic Peninsula Ice Sheet—can induce instrument vibrations and generate spurious precipitation signals. Consequently, the moderate correlations should not be interpreted solely as a limitation of MAR, but rather as a manifestation of the uncertainties inherent to precipitation observations in this region.

The choice of threshold used to define intense events also influences the results. While several studies use the 90th or 95th percentiles to identify extremes (e.g., Garreaud, 2018; Turner et al., 2019; Demortier et al., 2021; Wang et al., 2021, 2022; González-Reyes et al., 2023; Simon et al., 2023; Zhang et al., 2025; Prokhorova et al., 2025), others adopt more restrictive thresholds such as the 99th percentile (e.g., Favier et al., 2025, in review). Here, we assessed the sensitivity of our results using these three thresholds. Applying the 90th and 95th percentiles for the identification of IWEs and IPEs reduces the number of compound day events moderately (from 127 to approximately 100), whereas the 99th percentile substantially reduces the sample to about 20 cases (Fig. S8a). Although threshold selection affects the sample size, the main synoptic patterns remain consistent whatever the threshold (Fig. S8b).

The identification of ARs represents an additional source of methodological uncertainty. Previous studies have shown that AR frequency and characteristics can vary substantially depending on the detection algorithm used (Guan and Waliser, 2024; Thaker et al., 2025; Buffet et al., 2026, in review). For instance, Buffet et al. (2026, in review) reported that their catalogue identifies fewer but more intense AR days compared to that of Guan and Waliser (2024) over the Antarctic Peninsula. This methodological sensitivity implies that the selection of AR catalogue may influence the frequency and number of compound events.

5.2 Atmospheric synoptic configuration

IWEs over the Patagonian Icefields have been consistently associated with a high-pressure system over Patagonia (Jacques-Coper et al., 2021; Demortier et al., 2021; González-Reyes et al., 2023; Collazo et al., 2024), whereas IPEs over the Antarctic Peninsula Ice Sheet are linked to a dipole circulation pattern characterized by an anticyclone over the Malvinas/Falkland Islands and a cyclone over the Bellingshausen Sea (Wang et al., 2021, 2022). Our results indicate that the co-occurrence of IWEs and IPEs with ARs is associated with a statistically significant amplification of this dipole pattern. A dipole index, defined as the difference between sea-level pressure anomalies over the Malvinas/Falkland Islands and the Bellingshausen Sea, is significantly larger during compound events than during IPEs alone (Fig. S9 with Mann–Whitney U test, $p < 0.001$), confirming that compound events occur under enhanced large-scale circulation anomalies.

https://doi.org/10.5194/egusphere-2026-3508
Preprint. Discussion started: 31 July 2026

One possible mechanism involves the interaction between ARs and the regional circulation over the Antarctic Peninsula. Previous studies have shown that latent heat release associated with intense moisture transport can enhance upper-level ridging and modify downstream circulation during the life cycle of ARs (e.g. Wille et al., 2024). In this context, diabatic heating associated with condensation within ARs may contribute to strengthening the anticyclonic ridge extending toward Patagonia while simultaneously deepening the Bellingshausen Sea cyclone. Such circulation changes would favor both anomalous warming over the Patagonian Icefields and enhanced precipitation over the Antarctic Peninsula Ice Sheet. Although this mechanism is physically consistent with our results, further analyses of thermodynamic budgets, diabatic heating rates, and upper-level circulation anomalies are required to quantify its contribution to the observed dipole amplification.

The schematic shown in Fig. 10 should be viewed as a conceptual summary of the circulation anomalies identified during compound events. The temporal evolution of sea-level pressure anomalies (see Fig. 5) indicates that compound events are preceded by a progressive deepening of the Amundsen–Bellingshausen Sea Low and a strengthening of anticyclonic anomalies over southern South America and the South Atlantic sector. Beyond the regional dipole, the circulation anomalies exhibit a broader wave-like structure extending across the South Pacific, consistent with a Pacific–South American (PSA)-like pattern (Irving and Simmonds, 2016). Previous studies have shown that PSA-related Rossby wave trains provide an important pathway through which tropical Pacific variability influences the Amundsen–Bellingshausen Sea Low and Antarctic climate. In this context, the intensified dipole identified during compound events may represent the regional expression of a larger-scale PSA-like circulation anomaly. Future work should quantify the relative contributions of PSA variability, ENSO forcing, and the SAM to the occurrence and intensity of these compound events.

https://doi.org/10.5194/egusphere-2026-3508
Preprint. Discussion started: 31 July 2026

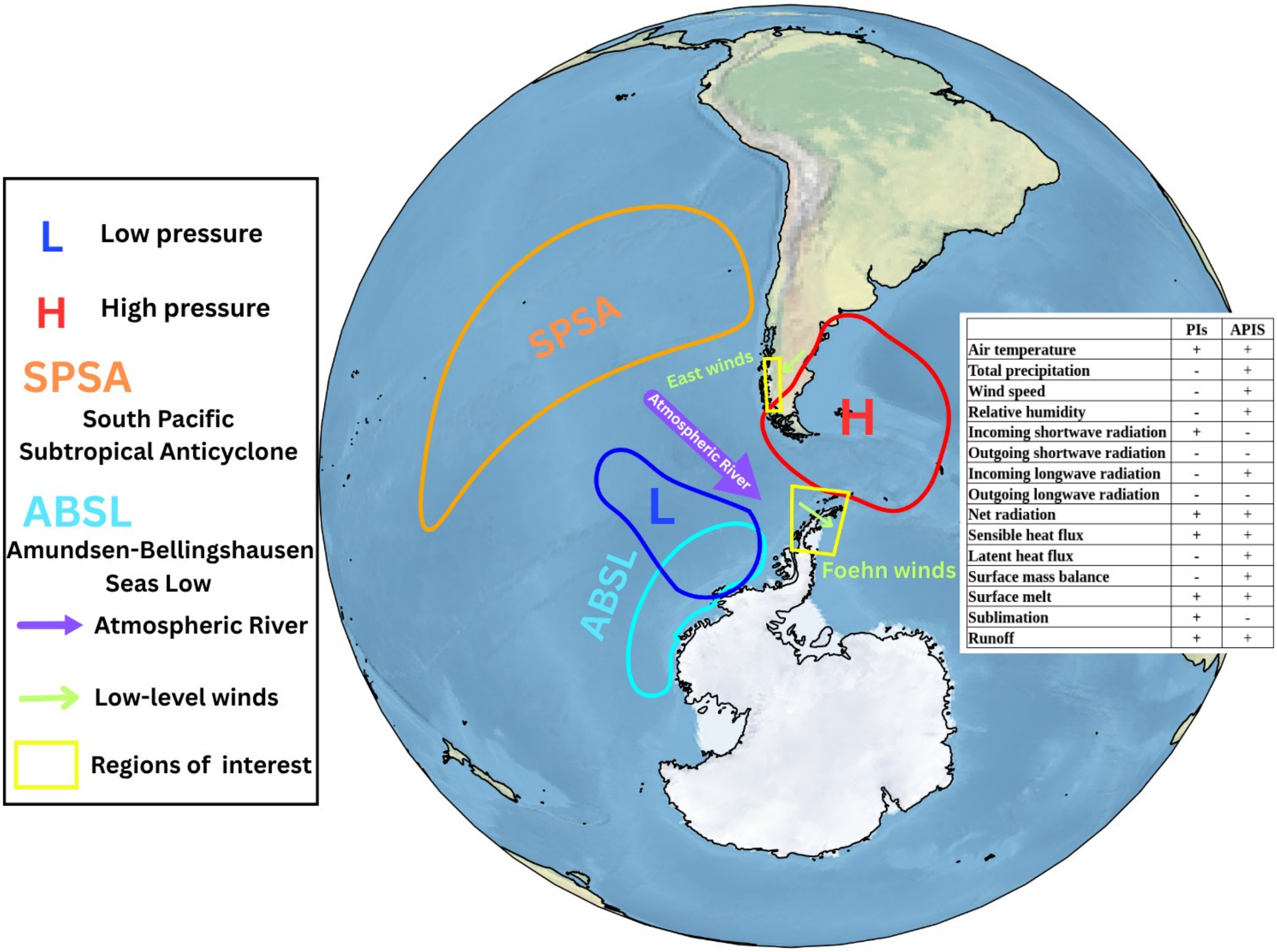

	PIs	APIS
Air temperature	+	+
Total precipitation	-	+
Wind speed	-	+
Relative humidity	-	+
Incoming shortwave radiation	+	-
Outgoing shortwave radiation	-	-
Incoming longwave radiation	-	+
Outgoing longwave radiation	-	-
Net radiation	+	+
Sensible heat flux	+	+
Latent heat flux	-	+
Surface mass balance	-	+
Surface melt	+	+
Sublimation	+	-
Runoff	+	+

Figure 10: Schematic overview of the atmospheric circulation pattern associated with the 127 days when IWEs, IPEs, and ARs occurred simultaneously over the Patagonian Icefields and the Antarctic Peninsula Ice Sheet, and their impacts on atmospheric and glaciological conditions. The climatological positions of the South Pacific Subtropical Anticyclone and the Amundsen–Bellingshausen Seas Low during austral summer, based on ERA5 data, are also shown. Plus (minus) signs indicate increases (decreases) in meteorological and glaciological variables over the Patagonian Icefields (PIs) and the Antarctic Peninsula Ice Sheet (APIS).

5.3 Glacier surface energy and mass balance impacts

Despite these advances, the links between large-scale circulation anomalies and glacier surface processes acting simultaneously over the Patagonian Icefields and the Antarctic Peninsula Ice Sheet remain incompletely understood. Previous studies indicate that net radiation and sensible heat flux dominate the surface energy balance (SEB), while latent

heat flux can either cool or warm glacier surfaces depending on regional conditions (Braun et al., 2001; Schneider, 1999; Bravo et al., 2022). Under certain large-scale configurations, particularly during dipole patterns with AR activity–turbulent heat fluxes can intensify and enhance melt and runoff (Zou et al., 2023; Gorodetskaya et al., 2023). However, AR events may also promote positive SMB when snowfall at higher elevations offsets melt (Wille et al., 2021; Maclennan et al., 2022).
In this context, our results highlight regionally distinct SEB responses during compound events. Over the Patagonian Icefields, surface warming is primarily driven by positive anomalies in incoming and net shortwave radiation, together with enhanced sensible heat flux, consistent with previous studies (e.g., Zhang et al., 2025; Prokhorova et al., 2025).
In contrast, over the Antarctic Peninsula Ice Sheet, the SEB is mainly controlled by increased incoming longwave radiation and sensible heat flux, favoring melt particularly at lower elevations. Despite this enhanced melt, SMB anomalies remain positive over large sectors, indicating that snowfall at higher elevations counterbalance the mass losses. This reflects the dual role of ARs, which promote rainfall in coastal areas while delivering substantial snowfall inland (Wille et al., 2021; Maclennan et al., 2022).
Negative SMB anomalies are primarily confined to the eastern Antarctic Peninsula Ice Sheet, where local processes such as foehn winds enhance sensible heat flux and amplify melt and sublimation, leading to localized mass losses (Bozkurt et al., 2018; Zou et al., 2023).

6 Conclusions

This study examines the atmospheric drivers and surface impacts of intense warming over the Patagonian Icefields and intense precipitation associated with atmospheric rivers over the Antarctic Peninsula Ice Sheet, with particular focus on their potential simultaneity.
The identification of these events using the Modèle Atmosphérique Régional model, supported by available observations, indicates that the model captures the interannual variability of intense warming events robustly and provides a reasonable representation of intense precipitation events despite observational uncertainties. While methodological choices affect events frequency, the main synoptic patterns remain consistent.
Intense warming over the Patagonian Icefields is linked to high-pressure systems over Patagonia, whereas intense precipitation over the Antarctic Peninsula is associated with a dipole configuration featuring an anticyclone over the Malvinas/Falkland Islands and a cyclone over the Bellingshausen Sea. The simultaneous occurrence of these events results from an intensification and favorable positioning of this dipole, which enhances both warm air advection and moisture transport.
At the surface, impacts differ between regions. Over the Patagonian Icefields, melt is primarily driven by shortwave radiation and sensible heat flux, while over the Antarctic Peninsula Ice Sheet, longwave radiation and sensible heat flux dominate. Despite enhanced melt, positive surface mass balance anomalies occur over the Antarctic Peninsula Ice Sheet due to increased snowfall at higher elevations, although localized mass losses are observed in regions affected by foehn winds.

https://doi.org/10.5194/egusphere-2026-3508
Preprint. Discussion started: 31 July 2026

Compound simultaneous events can contribute up to ~10% of ablation over the Patagonian Icefields, with negligible effects on accumulation, whereas over the Antarctic Peninsula Ice Sheet they account for up to ~20% of accumulation and less than ~15% of ablation, indicating a greater influence on surface mass balance across the peninsula.

Atmospheric river integrated water vapor transport intensity does not significantly modulate precipitation, surface energy balance and surface mass balance components over the Antarctic Peninsula Ice Sheet, indicating that these events are primarily governed by a large-scale dipole circulation pattern rather than integrated water vapor transport intensity alone.

Overall, these results emphasize the strong coupling between large-scale circulation, surface energy balance, and glacier mass response across Patagonia and the Antarctic Peninsula.

Code and data availability

ERA5 (Hersbach et al., 2020) data generated by ECMWF are available at the Climate Data Store (https://cds.climate.copernicus.eu/). The AR data were provided by Bin Guan via https://dataverse.ucla.edu/dataverse/ar. Hourly meteorological observation data at Palmer Station are available from the Antarctic Meteorological Research and Data Center (https://doi.org/10.48567/0fzs-fy93). MAR model outputs and further data will be made available on request. All analyses and figures were produced using Python, with some edits made in Canva, and can be accessed at: https://github.com/cryohydromettools/PIs_APIS_Part1.

Supplement link

The link to the supplement will be included by Copernicus, if applicable.

Author contributions

CT curated and analyzed the data and prepared the initial draft of the manuscript, including figures and visualizations. DB and VF guided the investigation and contributed to refining the final version of the manuscript. VF performed the wave flux analysis and contributed to revising the final manuscript. CB provided observational data over the Patagonian Icefields and contributed to data analysis. XF provided MAR outputs over the Patagonian Icefields and contributed to revising the final manuscript. TD provided MAR outputs over the Antarctic Peninsula Ice Sheet and contributed to revising the final manuscript. AR contributed to revising the final manuscript. MV guided the processing of atmospheric river data and contributed to revising the final manuscript. SP provided data from King Sejong Station and contributed to reviewing and editing the final manuscript. JAN contributed to securing the financial support for the project leading to this publication and to revising the final manuscript.

https://doi.org/10.5194/egusphere-2026-3508
Preprint. Discussion started: 31 July 2026

Competing interests

At least one of the (co-)authors is a member of the editorial board of The Cryosphere.

Acknowledgements

This study was financed, in part, by the São Paulo Research Foundation (FAPESP), Brasil. Process Number 2025/12582-1. This work was carried out with the support of CAPES, Coordination for the Improvement of Higher Education Personnel, Brazil, within the scope of the CAPES/COFECUB Program (project number 88881.188771/2025-01, TROPIPOLAR-CRYOEXTREMES). This research was partially supported by the supercomputing infrastructure of the NLHPC (CCSS210001) (ECM-02:Powered@NLHPC). The data (KOPRI-KPDC-00000960) from King Sejong Station used in this work was provided by the Korea Polar Research Institute. SJ was supported by KOPRI grant funded by the Ministry of Oceans and Fisheries (PE26030). MAR computational resources have been provided by the Consortium des Équipements de Calcul Intensif (CÉCI), funded by the Fonds de la Recherche Scientifique de Belgique (F.R.S.-FNRS) under Grant No. 2.5020.11 and by the Walloon Region. Claudio Bravo received support from ANID grant FONDECYT Iniciación 11240379. Deniz Bozkurt acknowledges support from ANID-FONDECYT-1240190, COPAS COASTAL ANID FB210021 and ANID ANILLO ATE250008. Finally, we acknowledge OpenAI's ChatGPT which only was used to improve the text's quality English of the manuscript.

References

Aguayo, R., León-Muñoz, J., Aguayo, M., Baez-Villanueva, O. M., Zambrano-Bigiarini, M., Fernandez, A., and Jacques-Coper, M.: PatagoniaMet: A multi-source hydrometeorological dataset for Western Patagonia, Sci. Data, 11(1), 6, https://doi.org/10.1038/s41597-023-02828-2, 2024.

Bozkurt, D., Rondanelli, R., Marín, J. C., and Garreaud, R.: Foehn event triggered by an atmospheric river underlies record-setting temperature along continental Antarctica, J. Geophys. Res. Atmos., 123(8), 3871-3892, https://doi.org/10.1002/2017JD027796, 2018.

Bozkurt, D., Marín, J. C., and Barrett, B. S.: Temperature and moisture transport during atmospheric blocking patterns around the Antarctic Peninsula, Weather Clim. Extrem., 38, 100506, https://doi.org/10.1016/j.wace.2022.100506, 2022.

Bozkurt, D., Marín, J. C., Verdugo, C., and Barrett, B. S.: Atmospheric blocking and temperatures in the Antarctic Peninsula, Sci. Total Environ., 931, 172852, https://doi.org/10.1016/j.scitotenv.2024.172852, 2024a.

Bozkurt, D., Carrasco, J. F., Cordero, R. R., Fernandoy, F., Gómez-Contreras, A., Carrillo, B., and Guan, B.: Atmospheric river brings warmth and rainfall to the northern Antarctic Peninsula during the mid-austral winter of 2023, Geophys. Res. Lett., 51(13), e2024GL108391, https://doi.org/10.1029/2024GL108391, 2024b.

Buffet, V., Favier, V., Pohl, B., and Wille, J. D.: Curved atmospheric rivers and their moisture remnants: a new detection tool for Antarctica, EGUsphere, [preprint], https://doi.org/10.5194/egusphere-2025-6365, 9 January 2026.

Brun, E., David, P., Sudul, M., and Brunot, G.: A numerical model to simulate snow-cover stratigraphy for operational avalanche forecasting, J. Glaciol., 38(128), 13-22, https://doi.org/10.3189/S0022143000009552, 1992.

Bravo, C., Ross, A. N., Quincey, D. J., Cisternas, S., and Rivera, A. (2022). Surface ablation and its drivers along a west–east transect of the Southern Patagonia Icefield. Journal of Glaciology, 68(268), 305-318. https://doi.org/10.1017/jog.2021.92

Braun, M., Saurer, H., Vogt, S., Simões, J. C., and Goßmann, H. E. R. M. A. N. N.: The influence of large-scale atmospheric circulation on the surface energy balance of the King George Island ice cap, Int. J. Climatol., 21(1), 21-36, https://doi.org/10.1002/joc.563, 2001.

Carrasco, J. F., Bozkurt, D., and Cordero, R. R.: A review of the observed air temperature in the Antarctic Peninsula. Did the warming trend come back after the early 21st hiatus?, Polar Sci., 28, 100653, https://doi.org/10.1016/j.polar.2021.100653, 2021.

Carrasco, J. F., and Cordero, R. R.: Analyzing precipitation changes in the northern tip of the Antarctic Peninsula during the 1970–2019 period, Atmosphere, 11(12), 1270, https://doi.org/10.3390/atmos11121270, 2020.

Carrasco-Escaff, T., Rojas, M., Garreaud, R. D., Bozkurt, D., and Schaefer, M. Climatic control of the surface mass balance of the Patagonian Icefields, Cryosphere, 17(3), 1127-1149, https://doi.org/10.5194/tc-17-1127-2023, 2023.

Clem, K. R., Bozkurt, D., Kennett, D., King, J. C., and Turner, J.: Central tropical Pacific convection drives extreme high temperatures and surface melt on the Larsen C Ice Shelf, Antarctic Peninsula, Nat. Commun., 13(1), 3906, https://doi.org/10.1038/s41467-022-31119-4, 2022.

Cook, A. J., Holland, P. R., Meredith, M. P., Murray, T., Luckman, A., and Vaughan, D. G.: Ocean forcing of glacier retreat in the western Antarctic Peninsula, Science, 353(6296), 283-286, https://doi.org/10.1126/science.aae0017, (2016).

Collao-Barrios, G., Favier, V., Gillet-Chaulet, F., Fettweis, X., Gallée, H., Santolaria-Otín, M., Davaze, L., and Raleigh, M. S.: Surface mass balance of the Northern Patagonian Ice Field and links with climate variability modes and atmospheric variables, J. Glaciol., 72, e9, https://doi.org/10.1017/jog.2025.10106, 2026.

Collazo, S., Suli, S., Zaninelli, P. G., García-Herrera, R., Barriopedro, D., and Garrido-Perez, J. M.: Influence of large-scale circulation and local feedbacks on extreme summer heat in Argentina in 2022/23, Commun. Earth Environ., 5(1), 231, https://doi.org/10.1038/s43247-024-01386-8, 2024.

Demortier, A., Bozkurt, D., and Jacques-Coper, M.: Identifying key driving mechanisms of heat waves in central Chile, Climate Dynamics, 57(9), 2415-2432, https://doi.org/10.1007/s00382-021-05810-z, 2021.

Dethinne, T., Glaude, Q., Picard, G., Kittel, C., Alexander, P., Orban, A., and Fettweis, X.: Sensitivity of the MAR regional climate model snowpack to the parameterization of the assimilation of satellite-derived wet-snow masks on the Antarctic Peninsula, Cryosphere, 17(10), 4267-4288, https://doi.org/10.5194/tc-17-4267-2023, 2023.

https://doi.org/10.5194/egusphere-2026-3508
Preprint. Discussion started: 31 July 2026

Dunn, R. E., Fowler, H. J., Green, A. C., and Lewis, E.: Tipping-bucket rain gauges: A review of the undercatch phenomenon, and methods for its reduction and correction, Weather, 80(6), 196-205, https://doi.org/10.1002/wea.7736, 2025.

Favier, V., Blanchet, J., Dutrievoz, N., Pohl, B., Clem, K., Barthelemy, L., Buffet, V., Wille, J., Codron, F., Bozkurt, B., Baiman, R., Winters, A., Gorodetskaya, I., Vance, T., and Udy, D.: Extreme temperature trends in Antarctica exacerbated by explosive atmospheric rivers, [preprint], https://doi.org/10.21203/rs.3.rs-7706789/v1, 10 November 2025.

Fettweis, X., Hofer, S., Séférian, R., Amory, C., Delhasse, A., Doutreloup, S., Kittel, C., Lang, C., Van Bever, J., Veillon, F., and Irvine, P.: Brief communication: Reduction in the future Greenland ice sheet surface melt with the help of solar geoengineering, Cryosphere, 15(6), 3013-3019, https://doi.org/10.5194/tc-15-3013-2021, 2021.

Fogt, R. L., and Marshall, G. J.: The Southern Annular Mode: variability, trends, and climate impacts across the Southern Hemisphere, Wiley Interdiscip. Rev.: Clim. Change., 11(4), e652, https://doi.org/10.1002/wcc.652, 2020.

Fürst, J. J., Farías-Barahona, D., Blindow, N., Casassa, G., Gacitúa, G., Koppes, M., Lodolo, E., Millan, R., Minowa, M., Mouginot, J., Pętlicki, M., Rignot, E., Rivera, A., Skvarca, P., Stuefer, M., Sugiyama, S., Uribe, J., Zamora, R., Braun, M., Gillet-Chaulet, F., Malz, P., Meier, W., and Schaefer, M.: The foundations of the Patagonian icefields, Commun. Earth Environ., 5(1), 142, https://doi.org/10.1038/s43247-023-01193-7, 2024.

Garreaud, R., López, P., Minvielle, M., and Rojas, M.: Large-scale control on the Patagonian climate, J. Clim., 26(1), 215-230. https://doi.org/10.1175/JCLI-D-12-00001.1, 2013.

Garreaud, R. D.: Record-breaking climate anomalies lead to severe drought and environmental disruption in western Patagonia in 2016, Climate Research, 74(3), 217-229. https://doi.org/10.3354/cr01505, 2018.

Garreaud, R. D., Jacques-Coper, M., Marín, J. C., and Narváez, D. A.: Atmospheric rivers in South-Central Chile: Zonal and tilted events, Atmosphere, 15(4), 406. https://doi.org/10.3390/atmos15040406, 2024.

Garcia-Santos, Y., Narvaez, D. A., Jacques-Coper, M., Saldías, G. S., Bozkurt, D., and Alessio, B. M.: Dominant wind patterns under the influence of atmospheric rivers: Implications for coastal upwelling off central-southern Chile, J. Geophys. Res. Oceans, 130(3), e2024JC021444, https://doi.org/10.1029/2024JC021444, 2025.

González-Herrero, S., Barriopedro, D., Trigo, R. M., López-Bustins, J. A., and Oliva, M.: Climate warming amplified the 2020 record-breaking heatwave in the Antarctic Peninsula, Commun. Earth Environ., 3(1), 122, https://doi.org/10.1038/s43247-022-00450-5, 2022.

Gorodetskaya, I. V., Durán-Alarcón, C., González-Herrero, S., Clem, K. R., Zou, X., Rowe, P., Rodriguez Imazio, P., Campos, D., Leroy-Dos Santos, C., Wille, J., Chyhareva, A., Favier, V., Blanchet, J., Pohl, B., Cordero, R., Park, S., Colwell, S., Lazzara, M., Carrasco, J., Gulisano, A., Krakovska, S., Ralph, M., Dethinne, T., and Picard, G.: Record-high Antarctic Peninsula temperatures and surface melt in February 2022: a compound event with an intense atmospheric river, npj Clim. Atmos. Sci., 6(1), 202, https://doi.org/10.1038/s41612-023-00529-6, 2023.

González-Reyes, Á., Jacques-Coper, M., Bravo, C., Rojas, M., and Garreaud, R.: Evolution of heatwaves in Chile since 1980, Weather Clim. Extrem., 41, 100588, https://doi.org/10.1016/j.wace.2023.100588, 2023.

Groff, D. V.: Palmer Station manual and automatic weather station observations 1989 to 2024, quality-controlled, adjusted, and gap-filled observational data, AMRDC Data Repository, accessed 2025-05-10, https://doi.org/10.48567/fwgs-n690, 2025.

Guan, B., and Waliser, D. E.: A regionally refined quarter-degree global atmospheric rivers database based on ERA5, Sci. Data., 11(1), 440, https://doi.org/10.1038/s41597-024-03258-4, 2024.

Hersbach, H., Bell, B., Berrisford, P., Hirahara, S., Horányi, A., Muñoz-Sabater, J., Nicolas, J., Peubey, C., Radu, R., Schepers, D., Simmons, A., Soci, C., Abdalla, S., Abellan, X., Balsamo, G., Bechtold, P., Biavati, G., Bidlot, J., Bonavita, M., De Chiara, G., Dahlgren, P., Dee, D., Diamantakis, M., Dragani, R., Flemming, J., Forbes, R., Fuentes, M., Geer, A., Haimberger, L., Healy, S., Hogan, R., Hólm, E., Janisková, M., Keeley, S., Laloyaux, P., Lopez, P., Lupu, C., Radnoti, G., de Rosnay, P., Rozum, I., Vamborg, F., Villaume, S., and Thépaut, J. N.: The ERA5 global reanalysis, Q. J. R. Meteorol. Soc., 146(730), 1999-2049, https://doi.org/10.1002/qj.3803, 2020.

Hosking, J. S., Orr, A., Marshall, G. J., Turner, J., and Phillips, T.: The influence of the Amundsen–Bellingshausen Seas low on the climate of West Antarctica and its representation in coupled climate model simulations, J. Clim., 26(17), 6633-6648, https://doi.org/10.1175/JCLI-D-12-00813.1, 2013.

Hoover, J., Earle, M. E., Joe, P. I., and Sullivan, P. E.: Unshielded precipitation gauge collection efficiency with wind speed and hydrometeor fall velocity, Hydrol. Earth Syst. Sci., 25(10), 5473-5491, https://doi.org/10.5194/hess-25-5473-2021, 2021.

Huss, M., and Farinotti, D.: A high-resolution bedrock map for the Antarctic Peninsula, Cryosphere, 8(4), 1261-1273, https://doi.org/10.5194/tc-8-1261-2014, 2014.

Irving, D., and Simmonds, I.: A new method for identifying the Pacific–South American pattern and its influence on regional climate variability, J. Clim., 29(17), 6109-6125. https://doi.org/10.1175/JCLI-D-15-0843.1, 2016.

Jacques Coper, M., Brönnimann, S., Martius, O., Vera, C. S., and Cerne, S. B.: Summer heat waves in southeastern Patagonia: an analysis of the intraseasonal timescale, Int. J. Climatol., https://doi.org/10.1002/joc.4430, 2016.

Kittel, C., Fettweis, X., Picard, G., and Gourmelen, N.: Assimilation of satellite-derived melt extent increases melt simulated by MAR over the Amundsen sector (West Antarctica). Bulletin de la Société Géographique de Liège, 78, 87-99. https://doi.org/10.25518/0770-7576.6616, 2022.

The IMBIE team.: Mass balance of the Antarctic Ice Sheet from 1992 to 2017, Nature 558, 219–222, https://doi.org/10.1038/s41586-018-0179-y, 2018.

Li, X., Cai, W., Meehl, G. A., Chen, D., Yuan, X., Raphael, M., Holland, D., Ding, Q., Fogt, R., Markle, B., Wang, G., Bromwich, D., Turner, J., Xie, S., Steig, E., Gille, S., Xiao, C., Wu, B., Lazzara, M., Chen, X., Stammerjohn, S., Holland, P., Holland, M., Cheng, X., Price, S., Wang, Z., Bitz, C., Shi, J., Gerber, E., Liang, X., Goosse, H., Yoo, C., Ding, M., Geng, L., Xin, M., Li, C., Dou, T., Liu, C., Sun, W., Wang, X., and Song, C.: Tropical teleconnection impacts on Antarctic climate changes, Nat. Rev. Earth Environ., 2(10), 680-698, https://doi.org/10.1038/s43017-021-00204-5, 2021.

https://doi.org/10.5194/egusphere-2026-3508
Preprint. Discussion started: 31 July 2026

Liang, K., Wang, J., Luo, H., Clem, K. R., Zhong, R., and Yang, Q.: Regional extreme Antarctic sea-ice retreat linked to tropical forcing, Commun. Earth Environ., 7(1), 337, https://doi.org/10.1038/s43247-026-03488-x, 2026.

Lu, J., Vecchi, G. A., and Reichler, T.: Expansion of the Hadley cell under global warming, Geophys. Res. Lett., 34(6), https://doi.org/10.1029/2006GL028443, 2007.

Macha, J. M., Mackintosh, A. N., McCormack, F. S., Henley, B. J., McGregor, H. V., Van Dalum, C. T., and Purich, A.: How do extreme ENSO events affect Antarctic surface mass balance?, Cryosphere, 19(5), 1915-1935, https://doi.org/10.5194/tc-19-1915-2025, 2025.

Maclennan, M. L., Lenaerts, J. T., Shields, C., and Wille, J. D.: Contribution of atmospheric rivers to Antarctic precipitation, Geophys. Res. Lett., 49(18), e2022GL100585, https://doi.org/10.1029/2022GL100585, 2022.

Minowa, M., Skvarca, P., and Fujita, K.: Climate and surface mass balance at Glaciar Perito Moreno, southern Patagonia, J. Clim., 36(2), 625-641, https://doi.org/10.1175/JCLI-D-22-0294.1, 2023.

Minowa, M., Schaefer, M., Sugiyama, S., Sakakibara, D., and Skvarca, P.: Frontal ablation and mass loss of the Patagonian icefields, Earth Planet. Sci. Lett., 561, 116811, https://doi.org/10.1016/j.epsl.2021.116811, 2021.

Noël, B., Lhermitte, S., Wouters, B., and Fettweis, X.: Poleward shift of subtropical highs drives Patagonian glacier mass loss. Nat. Commun., 16(1), 3795, https://doi.org/10.1038/s41467-025-58974-1, 2025.

Park, S.J., Choi, T.J., and Kim, S.J.: Heat flux variations over sea ice observed at the coastal area of the Sejong Station, Antarctica, Asia-Pac. J. Atmos. Sci., 49(4), 443–450. https://doi.org/10.1007/s13143-013-0040-z, 2013.

Palmer Station Research Associate.: Palmer Station Automated Weather Data System observational data, 2001-present (ongoing), AMRDC Data Repository, [data set], https://doi.org/10.48567/0fzs-fy93, 2023.

Prokhorova, U. V., Terekhov, A. V., Demidov, V. E., Romashova, K. V., Barskov, K. V., Chechin, D. G., Vasilevich, I.I., Tretiakov, M.V., Ivanov, B.V., and Verkulich, S. R.: Impact of Extreme Weather Events on the Surface Energy Balance of the Low-Elevation Svalbard Glacier Aldegondabreen, Water, 17(2), 274, https://doi.org/10.3390/w17020274, 2025.

Ridder, K., and Gallée, H.: Land surface–induced regional climate change in southern Israel, J. Appl. Meteorol. Climatol., 37(11), 1470-1485, https://doi.org/10.1175/1520-0450(1998)037<1470:LSIRCC>2.0.CO;2, 1998.

Rignot, E., Rivera, A., and Casassa, G.: Contribution of the Patagonia Icefields of South America to sea level rise, Science, 302(5644), 434-437, https://doi.org/10.1126/science.1087393, 2003.

Seefeldt, M. W., Low, T. M., Landolt, S. D., and Nylen, T. H.: Remote and autonomous measurements of precipitation for the northwestern Ross Ice Shelf, Antarctica, Earth Syst. Sci. Data., 13(12), 5803-5817, https://doi.org/10.5194/essd-13-5803-2021, 2021.

Simon, S., Turner, J., Thamban, M., Wille, J. D., and Deb, P.: Spatiotemporal variability of extreme precipitation events and associated atmospheric processes over Dronning Maud Land, East Antarctica, J. Geophys. Res. - Atmos., 129(7), e2023JD038993, https://doi.org/10.1029/2023JD038993, 2024.

Souverijns, N., Gossart, A., Lhermitte, S., Gorodetskaya, I. V., Kneifel, S., Maahn, M., Bliven, F.L., and van Lipzig, N. P.: Estimating radar reflectivity-Snowfall rate relationships and their uncertainties over Antarctica by combining disdrometer and radar observations, Atmos. Res., 196, 211-223, https://doi.org/10.1016/j.atmosres.2017.06.001, 2017.

Schneider, C.: Energy balance estimates during the summer season of glaciers of the Antarctic Peninsula, Glob. Planet. Change., 22(1-4), 117-130, https://doi.org/10.1016/S0921-8181(99)00030-2, 1999.

Takaya, K., and Nakamura, H.: A formulation of a phase-independent wave-activity flux for stationary and migratory quasigeostrophic eddies on a zonally varying basic flow, J. Atmos. Sci., 58(6), 608-627, https://doi.org/10.1175/1520-0469(2001)058<0608:AFOAPI>2.0.CO;2, 2001.

Torres, C., Bozkurt, D., Carrasco-Escaff, T., Bolibar, J., and Arigony-Neto, J.: New insights on the interannual surface mass balance variability on the South Shetland Islands glaciers, northerly Antarctic Peninsula, Glob. Planet. Change., 239, 104506. https://doi.org/10.1016/j.gloplacha.2024.104506, 2024.

Torres, C., Bozkurt, D., Matějka, M., Láska, K., Simon, S., Jaña, R., and Arigony-Neto, J.: Contrasting impacts of two mesoscale cyclones on the South Shetland Islands' glaciers, northern Antarctic Peninsula, Q. J. R. Meteorol. Soc., 151(772), e5052, https://doi.org/10.1002/qj.5052, 2025.

Turner, J., Lu, H., White, I., King, J. C., Phillips, T., Hosking, J. S., Bracegirdle, T., Marshall, G., Mulvaney, R., and Deb, P.: Absence of 21st century warming on Antarctic Peninsula consistent with natural variability, Nature, 535(7612), 411-415. https://doi.org/10.1038/nature18645, 2016.

Turner, J., Phillips, T., Thamban, M., Rahaman, W., Marshall, G. J., Wille, J. D., Favier, V., Winton, V., Thomas, E., Wang, Z., van den Broeke, M., Hosking, J. and Lachlan-Cope, T.: The dominant role of extreme precipitation events in Antarctic snowfall variability, Geophys. Res. Lett., 46(6), 3502-3511, https://doi.org/10.1029/2018GL081517, 2019.

Turner, J., Marshall, G. J., Clem, K., Colwell, S., Phillips, T., and Lu, H.: Antarctic temperature variability and change from station data, Int. J. Climatol., 40(6), 2986-3007, https://doi.org/10.1002/joc.6378, 2020.

Thaker, R., Vavrus, S. J., Shields, C. A., DuVivier, A. K., Maclennan, M., Holland, M. M., and Landrum, L.: Arctic atmospheric rivers in a changing climate and the impacts on sea ice, J. Geophys. Res. - Atmos., 130(10), e2024JD042521, https://doi.org/10.1029/2024JD042521, 2025.

Viale, M., Valenzuela, R., Garreaud, R. D., and Ralph, F. M.: Impacts of atmospheric rivers on precipitation in southern South America, J. Hydrometeor., 19(10), 1671-1687, https://doi.org/10.1175/JHM-D-18-0006.1, 2018.

Xu, M., Yu, L., Liang, K., Vihma, T., Bozkurt, D., Hu, X., and Yang, Q.: Dominant role of vertical air flows in the unprecedented warming on the Antarctic Peninsula in February 2020, Commun. Earth Environ., 2(1), 133, https://doi.org/10.1038/s43247-021-00203-w, 2021.

Wang, S., Liu, G., Ding, M., Chen, W., Zhang, W., and Lv, J.: Potential mechanisms governing the variation in rain/snow frequency over the northern Antarctic Peninsula during austral summer, Atmos. Res., 263, 105811. https://doi.org/10.1016/j.atmosres.2021.105811, 2021.

https://doi.org/10.5194/egusphere-2026-3508
Preprint. Discussion started: 31 July 2026

Wang, S., Ding, M., Liu, G., and Chen, W.: Processes and mechanisms of persistent extreme rainfall events in the Antarctic Peninsula during austral summer, J. Clim., 35(12), 3643-3657. https://doi.org/10.1175/JCLI-D-21-0834.1, 2022.

Wang, S., Liu, J., Cai, W., Yang, D., Kerzenmacher, T., Ding, S., and Cheng, X.: Strong impact of the rare three-year La Niña event on Antarctic surface climate changes in 2021–2023, npj Clim. Atmos. Sci., 8(1), 173. https://doi.org/10.1038/s41612-025-01066-0, 2025.

Welhouse, L. J., Lazzara, M. A., Keller, L. M., Tripoli, G. J., and Hitchman, M. H.: Composite analysis of the effects of ENSO events on Antarctica, J. Clim., 29(5), 1797-1808, https://doi.org/10.1175/JCLI-D-15-0108.1, 2016.

Wille, J. D., Favier, V., Gorodetskaya, I. V., Agosta, C., Kittel, C., Beeman, J. C., Jourdain, N., Lenaerts, J., and Codron, F.: Antarctic atmospheric river climatology and precipitation impacts, J. Geophys. Res. - Atmos., 126(8), e2020JD033788, https://doi.org/10.1029/2020JD033788, 2021.

Wille, J. D., Favier, V., Jourdain, N. C., Kittel, C., Turton, J. V., Agosta, C., Gorodetskaya, I., Picard, G., Codron, F., Santos, C., Amory, C., Fettweis, X., Blanchet, J., Jomelli, V., and Berchet, A.: Intense atmospheric rivers can weaken ice shelf stability at the Antarctic Peninsula, Commun. Earth Environ., 3, 90. https://doi.org/10.1038/s43247-022-00422-9, 2022.

Wille, J. D., Pohl, B., Favier, V., Winters, A. C., Baiman, R., Cavallo, S. M., Leroy-Dos Santos, C., Clem, K., Udy, D., Vance, T., Gorodetskaya, I., Codron, F., and Berchet, A.: Examining atmospheric river life cycles in East Antarctica, J. Geophys. Res. - Atmos., 129(8), e2023JD039970, https://doi.org/10.1029/2023JD039970, 2024.

Zhang, Q. L., Ding, M. H., Van Den Broeke, M. R., NoËl, B., Fettweis, X., Wang, S., Sun, W., You, Q. J., Xiao, C. Qin, D., and Huai, B. J.: Variations in Greenland surface melt and extreme events from 1958 to 2023, Adv. Clim. Change Res., 16(5), 910-921. https://doi.org/10.1016/j.accre.2025.05.004, 2025.

Zou, X., Rowe, P. M., Gorodetskaya, I., Bromwich, D. H., Lazzara, M. A., Cordero, R. R., Wille, J., Ralph, M., and Bai, L. S.: Strong warming over the Antarctic Peninsula during combined atmospheric river and foehn events: contribution of shortwave radiation and turbulence, J. Geophys. Res. - Atmos., 128(16), e2022JD038138, https://doi.org/10.1029/2022JD038138, 2023.